To appear in *The Astrophysical Journal* 10 July 1996

Cosmological Blastwaves and the Intergalactic Medium

G. Mark Voit[1,2]
Department of Physics and Astronomy, The Johns Hopkins University, Baltimore, MD 21218

ABSTRACT

Winds from protogalactic starbursts and quasars can drive shocks that heat, ionize, and enrich the intergalactic medium. The Sedov-Taylor solution for point-like explosions adequately describes these blastwaves early in their development, but as the time since the explosion ($t - t_1$) approaches the age of the universe (t), cosmological effects begin to alter the blastwave's structure and growth rate. This paper presents an analytical solution for adiabatic blastwaves in an expanding universe, valid when the IGM is homogeneous and contains only a small fraction of the total mass density ($\Omega_{\rm IGM} \ll \Omega_0$). In a flat universe, the solution applies until the age of the universe approaches $t_1 \Omega_{\rm IGM}^{-3/2}$, at which time the self-gravity of the matter associated with the shock compresses the shocked IGM into a thin shell. When $\Omega_{\rm IGM} \lesssim 0.03$, blastwaves starting after $z \sim 7$ and containing more than 10^{57} erg remain adiabatic to relatively low z, so this solution applies over a wide range of the parameter space relevant to galaxy formation. Using this analytical solution, we examine the role protogalactic explosions might play in determining the state of intergalactic gas at $z \sim 2 - 4$. Since much of the initial energy in galaxy-scale blastwaves is lost through cosmological effects, photoionization by a protogalaxy is much more efficient than shock ionization. Shocking the entire IGM by $z \sim 4$, when it appears to be substantially ionized, is most easily done with small explosions ($\lesssim 10^{56}$ erg) having a high comoving number density ($\gtrsim 1\,{\rm Mpc}^{-3}$). Larger-scale explosions could also fill the entire IGM, but if they did so, they would raise the mean metallicity of the IGM well above the levels observed in Lyα clouds. Since the metal abundances of Lyα clouds are small, the metals in these clouds were probably produced in small-scale bursts of star formation, rather than in large-scale explosions. The H I column densities of protogalactic blastwaves are much smaller than those of typical Lyα clouds, but interactions between shocks and preexisting Lyα clouds can potentially amplify the neutral column densities of preexisting clouds by a large factor.

Subject headings: galaxies: intergalactic medium — galaxies: quasars: absorption lines — ISM: supernova remnants — shock waves

---

[1]Hubble Fellow

[2]Current Address: STScI, 3700 San Martin Drive, Baltimore, MD 21218

1. Introduction

Gravity initiates the formation of galaxies in the early universe, but shortly thereafter, explosions, winds, and ionizing radiation from massive stars and active galactic nuclei complicate the hydrodynamics of galaxy formation and regulate the transformation of gas into stars (see recent reviews by Bond 1993 and Shapiro 1995). In the nearby universe we see starbursting galaxies expelling up to 10^{59} erg of thermal and kinetic energy into intergalactic space over the lifetime of the burst (see Heckman, Lehnert, & Armus 1993 for a review). The explosive output from a protogalaxy could be even larger, if most of its stars formed on the dynamical timescale of the galaxy.

Once the hot gas from a starburst escapes its host it flows into the intergalactic medium (IGM), shocking it, and eventually forming a blastwave similar to a supernova remnant. Because cosmological effects, such as the expansion of the universe, eventually govern their behavior, the explosions that emanate from quasars or protogalaxies have sometimes been called cosmological blastwaves. As these shocks pass through intergalactic space, they compress the IGM, sweeping it into denser sheets. Such a picture has naturally motivated suggestions that cosmological blastwaves are somehow related to the intergalactic Lyα clouds whose absorption signatures striate the spectra of high-redshift quasars (Ozernoi & Chernomordik 1978; Ostriker & Cowie 1981; Chernomordik & Ozernoi 1983; Ikeuchi & Ostriker 1986; Vishniac & Bust 1987).

Early treatments of cosmological blastwaves posited a baryonic IGM that dominated the matter content of the universe (Schwarz, Ostriker, & Yahil 1975; Ostriker & Cowie 1981; Ikeuchi, Tomisaka, & Ostriker 1983; Bertschinger 1983). Today the most successful cosmological models assume baryons comprise a relatively small fraction of the universe's matter content. Since the older solutions do not apply, cosmological blastwaves and their impact on the IGM deserve a fresh look from a more contemporary perspective. Computational approaches to such "feedback" during galaxy formation, while rapidly growing more sophisticated, are still limited by numerical resolution (e.g. Cen & Ostriker 1993; Navarro & White 1993). Analytical approaches, like the one taken here, while simplistic and idealized, can be more flexible than numerical solutions and offer insights complementary to those gained from simulations. Here we demonstrate that, in a universe filled primarily with collisionless matter, the structure and growth rate of a cosmological blastwave can be determined analytically. This new analytical solution turns out to be handy for reassessing the significance of protogalactic shocks in the IGM.

The paper is organized as follows. Section 2 presents an analytical solution for adiabatic cosmological blastwaves, valid when the mass density of the IGM is gravitationally unimportant. This solution is directly analogous to the Sedov-Taylor solution for adiabatic supernova remnants. As long as the shock remains adiabatic, the postshock density does not exceed four times the ambient intergalactic density until the shell of collisionless matter that collects at the shock front becomes self-gravitating. Section 3 discusses how ionizing radiation modifies the medium into which intergalactic shocks propagate, and § 4 considers the validity of the fluid approximation

in the IGM. Section 5 explores the global impact of protogalactic shocks on the temperature and metallicity of the IGM and derives constraints on the number density and energy scale of blastwave sources. Section 6 examines possible relationships between intergalactic blastwaves and Lyα clouds, and § 7 recapitulates the important results.

2. Blastwave Development

Intergalactic shocks can have an enormous impact on the IGM. Early calculations assuming that the ratio of the IGM mass density to the total mass density of the universe ($\delta_{\rm IGM} \equiv \Omega_{\rm IGM}/\Omega_0$) was close to unity found that protogalactic blastwaves could fill the IGM, heating and ionizing it by redshift z of a few (Schwarz *et al.* 1975). Subsequent treatments attempting to resolve cosmological shock structure in more detail (Ikeuchi *et al.* 1983; Bertschinger 1983; Vishniac, Ostriker, & Bertschinger 1985) generally took $\delta_{\rm IGM} = 1$ and found that shocks in an IGM dominated universe formed dense shells. Ikeuchi *et al.* (1983) assumed that dense shells would also form when $\delta_{\rm IGM} \ll 1$. At late times this certainly happens. An explosion in the IGM at a time t_1 since the big bang creates a cavity within which the mass density is a fraction $1 - \delta_{\rm IGM}$ lower than the background density. In a flat universe ($\Omega = 1$), collisionless matter within the cavity gradually overtakes the shock front and forms a shell when the age of the universe is $\sim t_1 \delta_{\rm IGM}^{-3/2}$ (Bertschinger 1985). After this time, blastwave evolution asymptotically approaches the usual self-similar solutions in which t_1 can be neglected, and the shocked IGM collapses into a dense layer just behind the shock front (Ikeuchi *et al.* 1983; Bertschinger 1983). If $\delta_{\rm IGM} \ll 1$, most of the interesting interactions of protogalactic shocks with the IGM occur long before the blastwave reaches the asymptotic self-similar stage.

This section presents an analytical solution for adiabatic cosmological blastwaves valid when $\delta_{\rm IGM} \ll 1$ and $t \ll t_1 \delta_{\rm IGM}^{-3/2}$. Taking advantage of some similarity properties of cosmological expansion (see Shandarin 1980 or Shapiro, Struck-Marcell, & Melott 1983), one can transform the cosmological fluid equations into a form without an explicit Hubble flow or background density. When the adiabatic index, γ, of the IGM equals 5/3, the transformed fluid equations admit a solution analogous to the Sedov-Taylor solution for adiabatic supernova remnants in a homogeneous medium. This solution turns out to be widely applicable, since cosmological shocks at $z \lesssim 7$ tend to remain adiabatic. The solution breaks down when either cooling becomes important or perturbations in the collisionless background flow become large.

2.1. Analytical Solution

Self-similar solutions for cosmological blastwaves can be found straightforwardly when the age of the blastwave is much less than the current age of the universe or when the age of the blastwave

is infinitesimally close to the current age of the universe (see Ostriker & McKee 1988 for a review). In these cases, there is only one important timescale. The intermediate case has been considered unfit for self-similar treatment because both the current age of the universe (t) and the age of the blastwave ($t - t_1$) are important. However, when $\delta_{\rm IGM} \ll 1$ a self-similar solution for cosmological blastwaves exists if $\gamma = 5/3$ and the blastwave is adiabatic.

To find this solution, we begin with the Newtonian fluid equations, valid as long as the length scales are much smaller than the horizon of the universe and the velocities are non-relativistic:

$$\frac{\partial \rho}{\partial t} + \nabla \rho \mathbf{u} = 0 \tag{2-1}$$

$$\frac{\partial \mathbf{u}}{\partial t} + (\mathbf{u} \cdot \nabla)\mathbf{u} = -\nabla\Phi - \frac{1}{\rho}\nabla P \tag{2-2}$$

$$\nabla^2 \Phi = 4\pi G(\rho + \rho_G) \tag{2-3}$$

$$\frac{d\epsilon}{dt} = \frac{P}{\rho^2}\frac{d\rho}{dt} + \rho\mathcal{H} - \rho^2\Lambda \tag{2-4}$$

$$\epsilon = \frac{1}{\gamma - 1}\frac{P}{\rho} \quad . \tag{2-5}$$

Here, $\mathbf{r}$ is the coordinate vector, $\mathbf{u}$ is the corresponding velocity, P is the gas pressure, ϵ is the specific internal energy, ρ is the IGM mass density, and ρ_G is the mass density of collisionless (non-baryonic plus condensed baryonic) matter. The undisturbed IGM comoves with the Hubble flow. Deviations from this flow can be expressed as a peculiar velocity field $\mathbf{v} = \mathbf{u} - H(t)\mathbf{r}$ under the influence of a perturbed potential field $\phi = \Phi - 2\pi G\bar{\rho}(t)r^2/3$. In terms of the scale factor $a(t) = [1 + z(t)]^{-1}$, which obeys $\dot{a}/a = H(t)$, the mean mass density is $\bar{\rho}(t) = \rho_0 a^{-3}(t)$, where $\rho_0 = \rho_{\rm cr}\Omega_0 = 3H_0^2\Omega_0/8\pi G$ is the mass density of the universe at the present time (t_0).

A transformation originally applied by Shandarin (1980) recasts the cosmological fluid equations into a very useful form (see also Shapiro *et al.* 1983). The transformed variables are:

$$d\hat{t} = a^{-2}dt \quad , \quad \hat{\mathbf{r}} = a^{-1}\mathbf{r} \quad , \quad \hat{\mathbf{v}} = a\mathbf{v} \quad , \quad \hat{\rho} = a^3\rho$$

$$\hat{P} = a^5 P \quad , \quad \hat{\epsilon} = a^2\epsilon \quad , \quad \hat{\phi} = a^2\phi \quad . \tag{2-6}$$

These variables obey the equations

$$\frac{\partial \hat{\rho}}{\partial \hat{t}} + \hat{\nabla}\hat{\rho}\hat{\mathbf{v}} = 0 \tag{2-7}$$

$$\frac{\partial \hat{\mathbf{v}}}{\partial \hat{t}} + (\hat{\mathbf{v}} \cdot \hat{\nabla})\hat{\mathbf{v}} = -\hat{\nabla}\hat{\phi} - \frac{1}{\hat{\rho}}\hat{\nabla}\hat{P} \tag{2-8}$$

$$\hat{\nabla}^2\hat{\phi} = 4\pi G(\hat{\rho} + \hat{\rho}_G - \rho_0)a \tag{2-9}$$

$$\frac{d\hat{\epsilon}}{d\hat{t}} = \frac{\hat{P}}{\hat{\rho}^2}\frac{d\hat{\rho}}{d\hat{t}} + (5 - 3\gamma)\left(\frac{1}{a}\frac{da}{d\hat{t}}\right)\hat{\epsilon} + \hat{\rho}a\mathcal{H} - \hat{\rho}^2 a^{-2}\Lambda \tag{2-10}$$

$$\hat{\epsilon} = \frac{1}{\gamma - 1}\frac{\hat{P}}{\hat{\rho}} \quad . \tag{2-11}$$

The form of these equations closely follows that of the initial set except that $\hat{r}$ and $\hat{v}$ now represent comoving positions and peculiar velocities.

When $\delta_{\rm IGM} \ll 1$, perturbations in the IGM have little effect on the underlying gravitational potential. If we also assume that the underlying collisionless matter is distributed effectively homogeneously on the scale of the blastwave, terms containing $\hat{\phi}$ can be ignored. In an adiabatic shock, the heating and cooling terms are negligible. The only term remaining that depends on cosmic time is the second term in the energy equation, which vanishes if $\gamma = 5/3$. This term accounts for the change in $\hat{\epsilon}$ that arises when ϵ does not vary as a^{-2}. In a monatomic gas, all the internal energy is in translational degrees of freedom. These atomic motions can be viewed as peculiar velocities that redshift away like a^{-1}, so that $\epsilon \propto a^{-2}$ in the absence of heating, cooling, and noncosmological work. Energy contained in rotational and other internal degrees of freedom does not redshift away and adds to $\hat{\epsilon}$ as the universe ages. Thus, in the transformed frame, the second term in the energy equation heats the gas when $\gamma > 5/3$.

The above equations are formally identical to the adiabatic fluid equations without cosmological and gravitational terms when $\mathcal{H} = \Lambda = \phi = 0$ and $\gamma = 5/3$. Since the time transformation involves only the time derivative, we are free to define $\hat{t} = 0$ to coincide with the cosmic time t_1 at which a galactic explosion (quasar or starburst) introduces an energy $E_0 = a^{-2}\hat{E}_0$ into the IGM. Solving for $\hat{t}(t)$ requires knowing $a(t)$ and thus Ω_0:

$$\hat{t} = \frac{2}{\Omega_0 H_0}[(1+\Omega_0 z_1)^{1/2} - (1+\Omega_0 z)^{1/2}] \ . \tag{2-12}$$

The standard Sedov self-similar solution (Sedov 1959, 1993) then satisfies the fluid equations, giving a shock radius of

$$\hat{R}_s = \left[\frac{\xi \hat{E}_0}{\hat{\rho}_{\rm IGM}}\right]^{1/5} \hat{t}^{2/5} \ , \tag{2-13}$$

where $\xi = 2.026$, $\hat{\rho}_{\rm IGM} = \rho_{\rm cr}\Omega_{\rm IGM}$ and $\Omega_{\rm IGM} \equiv \Omega_0\delta_{\rm IGM}$. At early times, $\hat{t} \approx (1+z_1)^2(t-t_1)$, and the shock radius in physical coordinates is

$$R_s = \left[\frac{\xi E_0}{\rho_0 \Omega_{\rm IGM}(1+z_1)^3}\right]^{1/5} (t-t_1)^{2/5} \ , \tag{2-14}$$

as expected. At large times, $\hat{t}$ asymptotically approaches a constant, so $\hat{R}_s$ approaches a constant comoving radius. The complete solution for the shock radius is

$$\begin{aligned} R_s &= \left[\frac{32\pi\xi G E_0}{3H_0^4\Omega_{\rm IGM}}\frac{(1+\Omega_0 z_1)}{\Omega_0^2(1+z_1)^2}\right]^{1/5}\left[1-\left(\frac{1+\Omega_0 z}{1+\Omega_0 z_1}\right)^{1/2}\right]^{2/5}(1+z)^{-1} \qquad (2\text{-}15)\\ &= (7.5\,{\rm Mpc})\left[\frac{1+\Omega_0 z_1}{\Omega_0^2(1+z_1)^2}\right]^{1/5} E_{61}^{1/5} h_{50}^{-4/5}\Omega_{\rm IGM}^{-1/5}\left[1-\left(\frac{1+\Omega_0 z}{1+\Omega_0 z_1}\right)^{1/2}\right]^{2/5}(1+z)^{-1} \ , \end{aligned}$$

where $E_{61} = E_0/(10^{61}\,\mathrm{erg})$. This solution is also valid when $\Omega_{\mathrm{IGM}} = \Omega_0 \ll z_1^{-1}$ because the gravitation of the collisionless matter is insignificant in this limit.

Since $\Omega_{\mathrm{IGM}} \ll 1$, the asymptotic radii of cosmological shocks can exceed 10 Mpc in comoving coordinates. Figure 1 shows how quickly the shock radius and shocked mass approach their asymptotic values in a flat universe. Voit (1994), solving for cosmological blastwave evolution in the thin-shell approximation, obtained an identical rate of convergence to the asymptotic solution. At the asymptotic radius, the blastwave has spent all the input energy in lifting the shocked IGM out of the gravitational potential of the collisionless matter interior to the shock. In the thin-shell approximation, the blastwave must lift all of the shocked IGM to the maximum radius, so the asymptotic radius in the thin-shell case is slightly smaller than in the exact solution.

2.2. Cooling

The onset of efficient cooling ends the adiabatic stage of blastwave development. Inverse Compton scattering of hot electrons off the cosmic microwave background cools cosmological shocks effectively at $z > 8h_{50}^{2/5} - 1$ in a flat universe. Radiative cooling is more important at lower redshifts but does not cool the shocked IGM very quickly. The cooling function $\Lambda(T)$ at temperature T in a low-metallicity plasma is of order $10^{-23}\,\mathrm{erg\,cm^3\,s^{-1}}$ for $10^5\,\mathrm{K} < T < 10^8\,\mathrm{K}$ (e.g. Sutherland & Dopita 1993; Schmutzler & Tscharnuter 1993). Just behind a strong shock front, the hydrogen number density n_{H} is four times the ambient IGM hydrogen density and the gas temperature is $T = 3\mu v_s^2/16k$, where v_s is the shock velocity relative to the Hubble flow and μ is the mean mass per particle. When the postshock cooling time $t_c = 5kT/n_{\mathrm{H}}\Lambda(T)$ is smaller than t, the current age of the universe, a cosmological shock is not adiabatic. If $\Omega_0 = 1$, cosmological shocks cool radiatively for

$$\begin{aligned} v_s &\lesssim \left[\frac{32}{15\pi}\frac{H_0\Omega_{\mathrm{IGM}}\Lambda}{Gm_p^2}\right]^{1/2}(1+z)^{3/4} \\ &\lesssim (77\,\mathrm{km\,s^{-1}})\Omega_{\mathrm{IGM}}^{1/2}\left(\frac{\Lambda}{10^{-23}\,\mathrm{erg\,cm^3\,s^{-1}}}\right)^{1/2} h_{50}^{1/2}\,(1+z)^{3/4}\,. \end{aligned} \tag{2-16}$$

If $\Omega_0 \ll z^{-1}$, the criterion for radiative cooling becomes

$$\begin{aligned} v_s &\lesssim \left[\frac{16}{5\pi}\frac{H_0\Omega_{\mathrm{IGM}}\Lambda}{Gm_p^2}\right]^{1/2}(1+z) \\ &\lesssim (96\,\mathrm{km\,s^{-1}})\Omega_{\mathrm{IGM}}^{1/2}\left(\frac{\Lambda}{10^{-23}\,\mathrm{erg\,cm^3\,s^{-1}}}\right)^{1/2} h_{50}^{1/2}\,(1+z)\,. \end{aligned} \tag{2-17}$$

Ionization losses can become important before radiative losses do. Blastwaves propagating into a neutral medium expend much of their energy collisionally ionizing the neutral gas when

$v_s \sim 40 - 80\,\mathrm{km\,s^{-1}}$. However, ultraviolet photons from the protogalaxy or quasar driving the blastwave are likely to preionize the IGM into which the shock propagates (§ 3).

The analytical solution of § 2.1 straightforwardly gives the velocity at the leading edge of an adiabatic shock:

$$\begin{aligned} v_s &= \frac{2}{5}\left[\frac{\pi\xi G H_0 E_0}{3\Omega_{\rm IGM}}\frac{\Omega_0^3(1+z_1)^3}{(1+\Omega_0 z_1)^{3/2}}\right]^{1/5}\left[1-\left(\frac{1+\Omega_0 z}{1+\Omega_0 z_1}\right)^{1/2}\right]^{-3/5}\left(\frac{1+z}{1+z_1}\right) \qquad (2\text{-}18) \\ &= (75\,\mathrm{km\,s^{-1}})\left[\frac{\Omega_0^2(1+z_1)^2}{1+\Omega_0 z_1}\right]^{3/10} E_{61}^{1/5} h_{50}^{1/5}\Omega_{\rm IGM}^{-1/5}\left[1-\left(\frac{1+\Omega_0 z}{1+\Omega_0 z_1}\right)^{1/2}\right]^{-3/5}\left(\frac{1+z}{1+z_1}\right) \ . \end{aligned}$$

Note that $v_s(z)$ depends only on Ω_0, z_1, and the parameter combination $E_{61}h_{50}\Omega_{\rm IGM}^{-1}$. Figure 2 shows how v_s varies with z for various values of $E_{61}h_{50}\Omega_{\rm IGM}^{-1}$ and several different initial redshifts, assuming $\Omega_0 = 1$. The vertical line indicates where inverse Compton scattering is marginally effective in cooling intergalactic shocks. The effectiveness of radiative cooling depends on the density and metallicity of the ambient IGM. Metallicities of Lyα clouds are probably $\lesssim 10^{-2}$ times solar (Tytler & Fan 1994; Cowie *et al.* 1995). At these levels of enrichment, $\Lambda(T)$ is nearly equal to the cooling function for a metal-free plasma. Solid lines across the lower portion of Figure 2 show where $t_c \approx t$, according to the cooling functions of Sutherland & Dopita (1993), for a metallicity of 10^{-2} times solar and $\Omega_{\rm IGM} = 0.01$ and 0.03. The shocks described here do not cool via radiative processes as long as $v_s(z)$ lies to the right of the Compton cooling region and above the radiatively cooling region. For a wide range of parameters, cosmological blastwaves are adiabatic. The analytical solution derived here is therefore valid in many interesting cases.

Once cooling becomes efficient, the blastwave grows more slowly than in the adiabatic case. If the shock cools radiatively, but the interior does not, then $\hat{E}_0 \propto \hat{R}_s^{-2}$ and $\hat{R}_s \propto \hat{t}^{2/7}$. This case is directly analogous to the pressure-driven snowplow solution for supernova remnants. If both the shock and the interior of the blastwave radiate efficiently, then blastwave momentum is constant in the transformed frame ($\hat{E}_0 \propto \hat{R}_s\hat{t}^{-1}$) and $\hat{R}_s \propto \hat{t}^{1/4}$, as in the momentum-conserving snowplow solution for supernova remnants. For more on supernova-remnant solutions see Ostriker & McKee (1988).

Cooling reduces the ultimate radius of a cosmological blastwave and the total amount of mass it can shock. Let $\hat{R}_{\rm asy}$ be the asymptotic comoving radius of an adiabatic blastwave, and define $\eta \equiv \hat{R}_s/\hat{R}_{\rm asy}$. Suppose that at $\eta = \eta_c$ and $\hat{t} = \hat{t}_c$ the blastwave begins to cool efficiently and obeys $\hat{R}_s = \hat{R}_{\rm asy}\eta_c(\hat{t}/\hat{t}_c)^\beta$ thereafter. The new asymptotic comoving radius of this blastwave, after cooling, is $\hat{R}_{\rm asy}\eta_c^{1-5\beta/2}$. Relative to the adiabatic case, the asymptotic shocked mass is $\eta_c^{6/7}$ times smaller when $\beta = 2/7$ and $\eta_c^{9/8}$ times smaller when $\beta = 1/4$.

2.3. Gravitation of the Shocked Shell

Shock compression of the IGM creates a radial perturbation in the gravitational potential that can modify the interior structure of a cosmological blastwave. In transformed variables, the surface density of the shocked IGM shell is $\hat{\sigma} = H_0^2 \Omega_{\rm IGM} \hat{R}_s / 8\pi G$. Note that the form of equation (2-9) implies $\hat{G} = G(1+z)^{-1}$. Behind the shock, the gravitational pressure scale height in the transformed system is

$$\hat{\lambda}_g \sim \frac{1+z}{H_0^2 \Omega_{\rm IGM}} \frac{\hat{v}_s^2}{\hat{R}_s} \, . \tag{2-19}$$

Thus, the gravitational pressure scale height in physical space is

$$\lambda_g \sim \frac{1}{25\,\Omega_{\rm IGM}} \left(\frac{1+z}{1+z_1} \right) R_s \, , \tag{2-20}$$

when $\Omega = 1$. In the absence of gravity, the density scale height inside an adiabatic blastwave is $\sim R_s/12$, so self-gravity does not alter the radial density structure of the blastwave significantly until $\lambda_g \sim R_s/12$ at $t \sim t_1 \Omega_{\rm IGM}^{-3/2}$. Gravitational forces modify the radial pressure profile of an adiabatic cosmological blastwave somewhat earlier. Without gravity, the gas pressure at $r < 0.8\,R_s$ plateaus at $\sim 0.4\,P(R_s)$ (Sedov 1959, 1993). The gravitational potential of the shocked shell steepens this plateau when $\lambda_g \sim R_s$. We can always neglect the self-gravity of an adiabatic shock when $\Omega_{\rm IGM} \ll \Omega \ll 1$.

2.4. Fragmentation

Density perturbations in the swept-up shell of gas behind a cosmological shock can become gravitationally unstable, leading to fragmentation of the shell and possibly the formation of Lyα clouds or galaxies (e.g. Ostriker & Cowie 1981). However, when $\delta_{\rm IGM} \ll 1$, gas shells behind adiabatic shocks do not fragment until the response of the collisionless matter starts to govern the dynamics. Formation of condensed gaseous structures through shock fragmentation alone thus requires either shocks that cool radiatively or $\delta_{\rm IGM} \approx 1$.

Let us examine the development of density perturbations in the transformed variables when $\Omega_{\rm IGM} \ll \Omega_0 = 1$ and the shock is adiabatic. A density perturbation of wavelength $\hat{\lambda}$ in a gas shell with a characteristic sound speed $\hat{c}_s$ grows if the sound crossing time $\hat{\lambda}\hat{c}_s^{-1}$ exceeds the free-fall time $(\hat{\lambda}/\hat{G}\hat{\sigma})^{1/2}$ (Ostriker & Cowie 1981; Vishniac 1983; Voit 1988). Thus, the minimum timescale, in transformed coordinates, for postshock IGM density perturbations to grow gravitationally is $\hat{t}_g \sim \hat{c}_s / \hat{G}\hat{\sigma}$. While the shock remains adiabatic, $\hat{c}_s \approx 0.16\,\hat{R}_s/\hat{t}$, and $\hat{t}_G \sim 9(1+z)\Omega_{\rm IGM}^{-1} t_0^2 \hat{t}^{-1}$. Postshock perturbations do not grow significantly until $\hat{t} \sim 3(1+z)^{1/2}\Omega_{\rm IGM}^{-1/2} t_0$, which corresponds to the epoch in physical time when $t \sim t_1 \Omega_{\rm IGM}^{-3/2}$. At this late point in the development of the blastwave, we can no longer ignore the peculiar flow induced in the collisionless matter as the IGM is swept up.

This stability analysis can be formulated more rigorously following Vishniac (1983), who examined the behavior of spherical blastwaves in the thin-shell approximation. Applying Vishniac's formalism to the gravitational stability problem in transformed coordinates yields a similar growth time, $\hat{t}_g \approx \hat{c}_s/\pi\hat{G}\hat{\sigma}$, and the same qualitative result. If $\delta_{\rm IGM} \ll 1$, adiabatic cosmological shocks do not fragment gravitationally until the response of collisionless matter to the blastwave begins to drive the shock front.

Radiative cooling, when it finally becomes a significant energy sink, reduces $\hat{c}_s$, allowing gravitational instabilities to develop earlier, but isothermal shocks are subject to a disruptive dynamical overstability that operates much more quickly than gravitational collapse (Vishniac 1983; Bertschinger 1986). Ripples in the shocked shell induce transverse flows of gas from the leading regions of the shell to the trailing regions. As the surface density of the trailing regions grows, the trailing regions begin to overtake the leading regions, and the process reverses. When the overstability becomes nonlinear, weak shocks damp the transverse flows, staving off complete disruption of the main shock front (Grun *et al.* 1991; Mac Low & Norman 1994). Gravitational instabilities therefore proceed to grow roughly as expected.

2.5. Comparisons with Other Solutions

Since the pioneering work of Schwarz *et al.* (1975), several investigators have presented numerical and analytical solutions for cosmological blastwaves. Many of these treatments assume $\delta_{\rm IGM} = 1$ and are not valid when $\Omega_{\rm IGM} \ll \Omega_0$. At late times ($t \gg t_1\Omega_{\rm IGM}^{-3/2}$) in a flat universe filled with collisionless matter,

$$\begin{aligned} R_s &= 1.89\,(E_0 G)^{1/5} t^{4/5} \\ &= (4.4\,{\rm Mpc}) E_{61}^{1/5} (1+z)^{-6/5}\,. \end{aligned} \tag{2-21}$$

(Bertschinger 1985). If $\Omega_{\rm IGM} \lesssim 0.1$, this solution does not yet apply to blastwaves beginning after the era of Compton cooling ($z_1 < 7$), because the collisionless component has not yet responded fully to the motion of the IGM. Several workers have formulated approximate expressions for $R_s(t)$ in the important regime where $t \ll t_1\Omega_{\rm IGM}^{-3/2}$ and $\Omega_{\rm IGM} \ll \Omega_0 = 1$. Here we compare these expressions with the exact solution derived in § 2.1.

2.5.1. Shock Radius

Adiabatic cosmological blastwaves start as spherical Sedov shocks and then asymptotically approach a constant comoving radius before the collisionless matter drives R_s to the late-time

solution. Ozernoy & Chernomordik (1978) constructed an approximate expression for R_s by matching a Sedov solution at early times to the solution of Schwarz et al. (1975) at late times. This approximation is poor because it presumes that the collisionless component responds to the blastwave on a timescale $\sim t_1$. Vishniac & Bust (1987) introduced a correction factor to the Sedov solution that reproduces, with reasonable accuracy, the behavior of $R_s(z)$ in numerical models of adiabatic cosmological shocks (Vishniac *et al.* 1985) when $\Omega_{\rm IGM} \ll \Omega = 1$. Figure 3 shows how their approximation (VB87) compares with the exact solution of § 2.1 (V95) and the late-time self-similar solution of Bertschinger (B85) for $\Omega_{\rm IGM} = 0.1$ and 0.01. The corrected Sedov solution remains within 10% of the exact solution until $t \sim 100 t_1$, regardless of $\Omega_{\rm IGM}$. After this time, the slope of VB87 is similar to B85. The point of departure of VB87 from V95 should be later for $\Omega_{\rm IGM} = 10^{-2}$, indicating that the VB87 correction factor was derived from models with $\Omega_{\rm IGM} \sim 0.1$. Ostriker & McKee (1988) formulated an expression for blastwave expansion that can be compared more directly with the solution of § 2.1. They constructed an approximate solution for adiabatic blastwaves when $\Omega_{\rm IGM} \ll \Omega_0 = 1$ by matching a Sedov-Taylor solution at early times to a comoving shell solution at late times. The approximation of Ostriker & McKee (1988), labeled OM88 in Figure 3, agrees well with the exact solution until $(1+z_1)/(1+z) \sim 4$ and ultimately reaches a somewhat smaller comoving radius.

The asymptotic comoving radius ($\hat{R}_{\rm asy}$) of a blastwave solution in a flat universe dominated by collisionless matter depends upon E_0, $\Omega_{\rm IGM}$, z_1, H_0, and also on the form of $R_s(t)$. When the other parameters are equal, solutions that expand more slowly reach larger values of $\hat{R}_{\rm asy}$. This is why the V95 and OM88 solutions eventually differ. To see how the shock expansion rate affects $\hat{R}_{\rm asy}$, consider how the initial energy E_0 shifts from the IGM to the collisionless component, assuming that the shock sweeps the IGM into a thin shell. As an IGM shell of mass M overtakes a collisionless shell of mass dM_d, the gravitational energy of the collisionless shell increases by $GM\,dM_d/R_s$ and the gravitational energy of the IGM shell decreases by the same amount. In terms of $\eta(x) \equiv \hat{R}_s/\hat{R}_{\rm asy}$ and $x \equiv (1+z)/(1+z_1)$, we can write the energy transfer rate as

$$\frac{dE}{dx} = \frac{3\,H_0^4 \hat{R}_{\rm asy}^5 \Omega_{\rm IGM}(1+z_1)}{4\,G}\, x\eta^4\eta' \,. \tag{2-22}$$

The total amount of energy transferred approaches E_0 as $x \to 0$; hence,

$$\hat{R}_{\rm asy} = \left[\frac{4\,GE_0}{3\,H_0^4\Omega_{\rm IGM}(1+z_1)}\right]^{1/5} \left(-\int_0^1 x\eta^4\eta'\,dx\right)^{-1/5} \,. \tag{2-23}$$

From § 2.1 we have $\eta(x) = (1-x^{1/2})^{2/5}$ when $\Omega_0 = 1$, which leads to

$$\hat{R}_{\rm asy} = \left[\frac{40\,GE_0}{H_0^4\Omega_{\rm IGM}(1+z_1)}\right]^{1/5} \,. \tag{2-24}$$

This is identical to the result obtained by Voit (1994) in the thin-shell approximation. The value of $\hat{R}_{\rm asy}$ from § 2.1 is 11% larger than this because the IGM density in the exact solution falls off more gradually behind the shock front, slightly reducing the amount of gravitational energy

associated with a given asymptotic radius. Note that blastwaves starting at later times expand to larger comoving radii. Ostriker & McKee (1988) took

$$\eta(x) = \left[(1 - 0.66\,x^{3/2})(1 - x^{3/2})^2\right]^{1/5} \ , \tag{2-25}$$

which yields an asymptotic radius in the thin-shell approximation 16% smaller than that in equation (27). The actual asymptotic radius of the OM88 solution is 20% smaller than the value of $\hat{R}_{\rm asy}$ from § 2.1. Figure 3 shows that the OM88 form for $\eta(x)$ increases more rapidly at early times, transferring the initial energy to the dark matter sooner, when the energy needed to achieve a given comoving radius is larger.

2.5.2. Shock Velocity

Although the blastwave radii of the approximate solutions do not differ dramatically, the predicted shock velocities can be quite different at late times. Figure 4 displays the shock velocities corresponding to the approximations illustrated in Figure 3. Because the OM88 approximation approaches its asymptotic radius so quickly, the shock velocity drops off rapidly beyond $t \sim 4t_1$. In this approximation the shock cools prematurely. The VB87 approximation is more accurate and remains close to V95 until $t \sim 30t_1$ ($\sim \Omega_{\rm IGM}^{-3/2} t_1$ for $\Omega_{\rm IGM} = 0.1$.)

2.5.3. Postshock Density

Immediately behind the shock front the gas density is four times the current IGM density. Because the solution of § 2.1 is directly analogous to the Sedov solution, the postshock density drops as r decreases. Gravitational forces can compress the shell further, but the compression does not become significant until $t \sim \Omega_{\rm IGM}^{-3/2} t_1$ (§ 2.3). Ikeuchi *et al.* (1981) argue that explosions in the IGM should eventually produce dense shells, but postshock densities in their numerical calculations do not exceed $4\rho_{\rm IGM}$ until $t \gtrsim 10t_1$.

3. Ionization

At $z < 5$, the intergalactic medium appears to be highly ionized (Gunn & Peterson 1965; Steidel & Sargent 1987; Webb *et al.* 1992; Giallongo *et al.* 1994). Blastwaves at these redshifts can expand adiabatically until radiative cooling limits their growth (§ 2.2). When the IGM is not

yet fully ionized, shocks initially propagate into a cosmological H II region created by ionizing radiation from the source of the blastwave, presumably a quasar or a protogalactic starburst. If the blastwave energy exceeds the ionizing output of the source, the shock can potentially enlarge the ionized cavity. Shocks reaching the neutral IGM at speeds greater than $\sim 50\,\mathrm{km\,s^{-1}}$ collisionally ionize additional gas. This section determines the conditions under which shock heating adds to the total mass of ionized gas.

Ultraviolet radiation from a quasar or starburst in the early universe quickly ionizes the surrounding IGM. Analytical models for the expansion of cosmological H II regions have been developed by Donahue & Shull (1987), Shapiro & Giroux (1987), and Madau & Meiksin (1991). The recombination time in a uniform IGM is $(6.3 \times 10^{10}\,\mathrm{yr})(1+z)^{-3}\Omega_{\rm IGM}^{-1}h_{50}^{-2}T_4^{0.8}$, where $T_4 = T/10^4\,\mathrm{K}$. Thus, at $z < 7$, ionized intergalactic gas with $\Omega_{\rm IGM} < 0.1$ remains predominantly ionized, and a burst of ionizing radiation produces a permanent H II region. Although the neutral fraction in this region does not necessarily remain small enough to satisfy existing constraints on the total optical depth of intergalactic Lyα, it does permit blastwaves to propagate at speeds slower than $80\,\mathrm{km\,s^{-1}}$ without suffering heavy ionization losses. If the central source emits $(10^{61}\,\mathrm{erg})E_{I61}$ in ionizing photons of average energy $(13.6\,\mathrm{eV})E_{\rm Ryd}$, the total gas mass of the ionized region is

$$M_I = (5.4 \times 10^{14}\,M_\odot)\,E_{I61}E_{\rm Ryd}^{-1}\,, \tag{3-1}$$

assuming primordial abundances. This mass corresponds to a comoving radius $\sim (12.3\,\mathrm{Mpc})E_{I61}^{1/3}E_{\rm Ryd}^{-1/3}h_{50}^{-2/3}\Omega_{\rm IGM}^{-1/3}$. The H II region grows much more rapidly than any hydrodynamic disturbance until the ionizing source shuts off and grows slowly thereafter as diffuse recombination radiation continues to provide ionizing photons. After the ionizing episode, the warm ionized gas can drive a $10 - 20\,\mathrm{km\,s^{-1}}$ shock into the neighboring neutral IGM. Madau & Meiksin (1991) employed a special case of the transformation described in § 2.1 in their analytical models of these shocks.

Collisional ionization adds to the ionized mass when the blastwave energy exceeds the radiative ionizing energy and the energy of the blastwave is relatively small. The mass of shocked gas inside an adiabatic cosmological blastwave is $M_{\rm asy}\eta^3$, where

$$\begin{aligned} M_{\rm asy} &= \frac{H_0^2\Omega_{\rm IGM}}{2\,G}\left[\frac{32\pi\xi GE_0}{3H_0^4\Omega_{\rm IGM}}\frac{(1+\Omega_0 z_1)}{\Omega_0^2(1+z_1)^2}\right]^{3/5} \\ &= (1.2\times10^{14}\,M_\odot)\left[\frac{1+\Omega_0 z_1}{\Omega_0^2(1+z_1)^2}\right]^{3/5}E_{61}^{3/5}h_{50}^{-2/5}\Omega_{\rm IGM}^{2/5} \end{aligned} \tag{3-2}$$

in a flat universe. Thus, an adiabatic blastwave eventually expands beyond the preionized region if

$$\frac{E_{I61}}{E_{61}} < 0.22\,E_{\rm Ryd}\left[E_{61}h_{50}\Omega_{\rm IGM}^{-1}\frac{\Omega_0^3(1+z_1)^3}{(1+\Omega_0 z_1)^{3/2}}\right]^{-2/5}\,. \tag{3-3}$$

Blastwaves generated by large-scale energy sources ($E_{61} \gtrsim 1$) remain within the preionized region unless the initial burst of ionizing radiation is quite weak. Smaller-scale blastwaves can escape

the preionized region more easily. The thermal energy density immediately behind a $\sim 50\,\mathrm{km\,s^{-1}}$ shock is just enough to ionize all the incoming hydrogen. Below this threshold, the postshock gas remains mostly neutral. Let η_I be the dimensionless comoving radius at which $v_s = 50\,\mathrm{km\,s^{-1}}$, so that $M_{\rm asy}\eta_I^3$ is the total mass of gas a cosmological blastwave can ionize. Figures 5 and 6 show how η_I and $M_{\rm asy}\eta_I^3$ depend on the parameter combination $E_{61}h_{50}(1+z_1)^{3/2}\Omega_{\rm IGM}^{-1}$ in a flat universe. Blastwaves in an open universe behave similarly.

When $\eta_I \ll 1$, a large proportion of the blastwave's energy can go into ionization of hydrogen. Small-scale blastwaves propagating into a neutral IGM lose significant energy to ionization when $v_s \sim 50 - 80\,\mathrm{km\,s^{-1}}$ and cool via Lyα when $v_s \sim 10 - 50\,\mathrm{km\,s^{-1}}$, as long as $\Omega_{\rm IGM} \gtrsim 0.01$. The blastwave switches from an adiabatic solution to a pressure-driven snowplow solution at $\eta = \eta_I$, so the total mass within the blastwave asymptotically approaches $M_{\rm asy}\eta_I^{6/7}$ (§ 2.2). In blastwaves with η_I approaching unity, most of the initial energy goes into the collisionless component when $\Omega_0 \approx 1$ or into kinetic energy that redshifts away when $\Omega_0 \ll 1$, leaving little available for ionization. Consequently, large-scale explosions are quite inefficient at ionizing the IGM.

Around quasars, photoionization exceeds collisional ionization. Although some quasars might expel winds with luminosities comparable to their radiative luminosities (Voit, Weymann, & Korista 1993), constraints on the distortion of the microwave background spectrum imply that the total energy in quasar blastwaves cannot exceed the total radiative output of quasars by a large factor (Voit 1994). Since the integrated radiative output of a typical quasar is $\sim 10^{61}\,\mathrm{erg}$, quasar blastwaves remain within their preionized cavities (see Fig. 6).

The ionizing properties of protogalaxies are harder to constrain because it is difficult to measure the fraction of ionizing photons that escape. In a starburst, the ratio of hydrodynamic to photoionizing output, integrated over the burst, can be as large as 0.3 (Leitherer & Heckman 1995). If the galaxy itself absorbs $> 70\%$ of the ionizing photons while allowing all of the hydrodynamic energy to escape, collisional ionization could, in principle, exceed photoionization in the surrounding IGM. For this to happen, the total magnitude of the protogalactic starburst would have to be quite small. If $\Omega_{\rm IGM} = 0.1$, $h_{50} = 1$, and $E_{I61}/E_{\rm Ryd}E_{61} = 0.3$, a blastwave beginning at $z_1 = 5$ would not augment the photoionized cavity unless $E_{61} < 10^{-4.7}$, implying $< 10^5$ supernovae.

4. Comments on the Fluid Approximation

Most investigations of intergalactic hydrodynamics, including this one, assume that the fluid equations adequately describe the behavior of the IGM, yet the mean free paths of fast particles in the IGM are not necessarily small. Coulomb collisions with electrons in a 10^4 K plasma stop a proton moving at $10^8\,v_8\,\mathrm{km\,s^{-1}}$ over an electron column density $\sim 10^{16}\,v_8^4\,\mathrm{cm^{-2}}$ (Spitzer 1962). This column corresponds to a comoving distance $\sim (0.1\,\mathrm{Mpc})(\Omega_{\rm IGM}/10^{-2})^{-1}v_8^4$. In a hot plasma

at $10^7\,T_7\,\mathrm{K}$, the column a proton traverses before Coulomb collisions significantly deflect it is $\sim 10^{17}\,T_7^2\,\mathrm{cm}^{-2}$ (Spitzer 1962), corresponding to a comoving distance $\sim (1\,\mathrm{Mpc})(\Omega_{\mathrm{IGM}}/10^{-2})^{-1}T_7^2$. These distances are similar to the length scales that emerge from cosmological blastwave solutions.

An intergalactic magnetic field of $10^{-20}\,B_{20}\,\mathrm{G}$ confines protons moving at $10^8\,v_8\,\mathrm{K}$ to within a gyroradius of $0.3\,v_8 B_{20}^{-1}\,\mathrm{Mpc}$, so a primordial field exceeding $10^{-19}\,\mathrm{G}$ would restore the fluid approximation on intergalactic scales. The actual strength of the intergalactic magnetic field is hard to constrain (Kronberg 1994). Because the current Galactic field ($\sim 10^{-6}\,\mathrm{G}$) must arise from an initially small seed field, some investigators have evaluated the primordial field strengths required by various models for Galactic field generation. Microwave background scattering inhibits the motions of electrons in rotating protogalaxies, causing the electrons to lag behind the ions. This weak current generates a small ($10^{-21}\,\mathrm{G}$) intergalactic field (Mishustin & Ruzmaikin 1972). Galactic dynamo action can potentially amplify a seed field this small by a factor $\sim e^{N_{\mathrm{rot}}} \sim 10^{15}$, where $N_{\mathrm{rot}} \sim 30$ is the number of times the Galaxy has rotated (Parker 1979). Kulsrud & Anderson (1992) have criticized this picture, arguing that is it very difficult for a galactic dynamo to create the current field from a very small seed field (but see Field 1995). The Galactic field would then have to arise from a much larger ($\sim 10^{-13}\,\mathrm{G}$) mean primordial field, amplifed primarily by the initial compression of the protogalactic gas.[1] Uncertain detections of Faraday rotation in radio-selected QSOs behind damped Lyα systems at $z \approx 2$ suggest that early galactic disks had fields $\sim 10^{-6}\,\mathrm{G}$ when $N_{\mathrm{rot}} \ll 30$ and would support the view that the intergalactic field must be $\gg 10^{-21}\,\mathrm{G}$ (Wolfe, Lanzetta, & Oren 1992).

In interstellar and interplanetary shocks, magnetic fields and plasma turbulence transfer energy between particles more efficiently than Coulomb collisions do, allowing postshock fluid structures to develop on length scales much shorter than the Coulomb mean free path (Draine & McKee 1993). Even in the absence of a magnetic field, electrostatic shocks mediated by plasma turbulence can thermalize the incoming particle energy in a distance similar to the Mach number times the Debye length (Tidman & Krall 1971). Since such shocks are quite thin, even in the IGM, the radii of cosmological blastwaves are still well defined and we can safely use the fluid equations and strong-shock jump conditions to describe how they propagate.

5. Global Effects

At redshift $z \approx 4$ the intergalactic medium is already highly ionized, and Lyα-absorbing clouds have formed. If cosmological blastwaves are responsible for maintaining the high ionization of the IGM or for producing Lyα clouds, they must have filled intergalactic space by this time. Hot electrons inside such blastwaves scatter microwave background photons, distorting the microwave

[1]Certain scenarios for inflation in the early universe can produce primordial fields as high as $10^{-9}\,\mathrm{G}$ (Ratra 1992).

background spectrum (Weymann 1965, 1966; Sunyaev & Zeldovich 1980). Limits on this distortion restrict the total blastwave energy density in the early universe. Metallicity limits further constrain the energy density in supernova blastwaves, if the metal abundances of Lyα clouds reflect the average metallicity of the IGM. The metallicity constraint allows adiabatic blastwaves beginning at $z_1 < 7$ to shock most of the IGM by $z \approx 4$ only if the energy per blastwave is small and the comoving number density of the blastwave sources is high ($\sim 1\,\mathrm{Mpc}^{-3}$). Thus, the metals in Lyα clouds were probably produced in small-scale starbursts ($< 10^{56}\,\mathrm{erg}$) rather than in large-scale protogalactic superwinds ($> 10^{57}\,\mathrm{erg}$). This section outlines these constraints in more detail.

5.1. Comptonization

The COBE satellite has shown that the cosmic microwave background spectrum deviates little from a pure blackbody. This lack of deviation can be used to limit the amount of energy injected into the IGM by cosmological blastwaves. Stars with a standard initial mass function release a fraction $\epsilon_{\mathrm{SN}} \sim 5 \times 10^{-6}$ of their initial rest mass energy in the form of kinetic energy from supernovae. The mean thermal energy density introduced into the IGM by supernovae in a star forming episode at z_1 is then

$$U_1(z_1) = (1.5 \times 10^{-14}\,\mathrm{erg\,cm^{-3}})(1+z_1)^3 h_{50}^2 f_{\mathrm{esc}} \Omega_* \ , \tag{5-1}$$

where f_{esc} is the fraction of the supernova energy that escapes a star-forming galaxy and Ω_* is the mass density of stars formed at z_1, in units of the critical density.[2] Since $\hat{E}_0$ is constant in adiabatic cosmological blastwaves, $U_1(z) = U_1(z_1)[(1+z)/(1+z_1)]^5$. Shocks in a low-density, preionized IGM remain adiabatic until z has changed significantly (Figure 2). The amount of y-distortion expected from such a star-forming episode is

$$y_1 \approx (2.2 \times 10^{-5})\, h_{50} f_{\mathrm{esc}} \Omega_* [(1+z_1)^{3/2} - (1+z_1)^{-2}] \ , \tag{5-2}$$

assuming $\Omega = 1$. COBE finds $y < 2.5 \times 10^{-5}$ at the 2σ level (Mather *et al.* 1994), implying $\Omega_* h_{50} f_{\mathrm{esc}} < 0.05 - 0.08$ for $z_1 = 7 - 5$. At $z_1 > 8 h_{50}^{2/5} - 1$ in a flat universe, Compton scattering transfers all the supernova energy to the microwave background, resulting in the limit $\Omega_* f_{\mathrm{esc}} < 2.8 \times 10^{-3}\,(1+z_1)$.

Fluctuations in the numbers of blastwaves along different lines of sight will cause the brightness of the microwave background to vary on small angular scales (Hogan 1984; Yoshioka & Ikeuchi 1987, 1988), but these fluctuations are relatively insignificant as long as the blastwave energies do not greatly exceed $10^{61}\,\mathrm{erg}$. A single blastwave distorts the microwave background by

[2] About 72% of the initial energy passes into thermal energy as the blastwave develops (Sedov 1959).

an amount

$$\Delta y \sim (9 \times 10^{-10}) \left[\frac{\Omega_0^2 (1+z_1)^2}{1+\Omega_0 z_1} \right]^{2/5} \left(\frac{1+z}{1+z_1} \right)^2 E_{61}^{3/5} h_{50}^{8/5} \Omega_{\rm IGM}^{2/5} \eta^{-2} \quad , \tag{5-3}$$

which reduces the background's brightness temperature by $\Delta T/T \approx -2\Delta y$. The temperature fluctuations induced by individual blastwaves are unobservable unless η is very small or E_{61} is very large.

Brightness temperature fluctuations from an ensemble of blastwaves depend upon how many blasts lie along a typical line of sight. The cross section of a blastwave is $\propto \eta^2$, but the amount of time a blastwave spends at a size $\eta \ll 1$ is $\propto \eta^{5/2}$. The number of blastwaves of size η along a line of sight is therefore $\mathcal{N}_\eta \propto \eta^{9/2}$. Large blastwaves contribute most heavily to y, so $\mathcal{N}_\eta(\eta \sim 1) \sim y/\Delta y$ and

$$\mathcal{N}_\eta < (3 \times 10^4) \left[\frac{\Omega_0^2 (1+z_1)^2}{1+\Omega_0 z_1} \right]^{-2/5} \left(\frac{1+z_1}{1+z} \right)^2 E_{61}^{-3/5} h_{50}^{-8/5} \Omega_{\rm IGM}^{-2/5} \eta^{9/2} \quad . \tag{5-4}$$

When there are many blasts along a line of sight, the y fluctuations from blasts of size η are $\sim \mathcal{N}_\eta^{1/2} \Delta y \propto \eta^{1/4}$. Blasts with $\eta \sim 1$ thus dominate the temperature fluctuations, which are of order

$$\frac{\Delta T}{T} < (3 \times 10^{-7}) \left[\frac{\Omega_0^2 (1+z_1)^2}{1+\Omega_0 z_1} \right]^{1/5} \left(\frac{1+z}{1+z_1} \right) E_{61}^{3/10} h_{50}^{4/5} \Omega_{\rm IGM}^{1/5} \quad . \tag{5-5}$$

The temperature fluctuations induced by galaxy-scale explosions, which cannot exceed $\sim 10^{-7}\, E_{61}^{3/10}$ for $z_1 \sim 5$ and $\Omega_{\rm IGM} \sim 0.01$, are presently unobservable.

Brightness temperature fluctuations imprinted by individual young ($\eta \ll 1$) blastwaves can exceed $\Delta T/T \sim 10^{-6}$, but these are rare. When $\Omega_{\rm IGM} \sim 0.01$, explosions with $\eta < 0.02 E_{61}^{3/10}$ can produce temperature fluctuations at this level. The angular sizes of such blasts at $z \sim 4$ in a flat universe would be $\sim 5\, E_{61}^{1/2}$ arcsec, and they would cover a fraction $< (3 \times 10^{-3}) E_{61}^{3/4}$ of the sky.

5.2. Metallicity

Supernova-driven winds from galaxies carry metals into intergalactic space, and the fraction of the metal-bearing supernova ejecta that escapes a starbursting galaxy should be $\sim f_{\rm esc}$. Since stars formed with a normal initial mass function eventually expel about 1% of the input mass in the form of metals, a star-formation episode enriches the IGM to a mean level $\sim f_{\rm esc} \Omega_* / \Omega_{\rm IGM}$ times solar metallicity. If the enrichments of Lyα clouds reflect average IGM abundances, then upper limits on the intergalactic metallicity constrain the energy input from supernova-driven blastwaves. Lu (1991) derived Lyα-cloud metallicities $\sim 10^{-3}$ times solar from stacked C IV spectra of clouds with neutral columns exceeding $N_{\rm H\,I} > 10^{15}\,{\rm cm}^{-2}$. Recent Keck spectra of

smaller clouds (Cowie *et al.* 1995) now indicate metallicities $\sim 10^{-2} - 10^{-2.5}$ times solar. Similar metallicities in the global IGM would imply $f_{\rm esc}\Omega_*/\Omega_{\rm IGM} \lesssim 10^{-2}$.

This constraint assumes that metals escaping from protogalaxies are evenly mixed into the IGM and Lyα clouds. The assumption of even mixing is most justifiable if protogalactic blastwaves filled the IGM before Lyα clouds condensed. If metal-bearing blasts encompassed only a small fraction of the IGM by the time Lyα clouds formed, the variance in intergalactic metallicities would be high. Enriched clouds would have high metallicities, while the others would be metal-free. Tytler & Fan (1994) determined that Lyα clouds with metallicities $\ll 10^{-2}$ times solar must be extremely rare, and Cowie *et al.* (1995) find a surprising consistency in cloud metallicities. While it is possible that the clouds are self-enriched by associated star formation (e.g. Cowie *et al.* 1995; Madau & Shull 1995) and do not reflect the metallicity of the IGM, they would still provide an upper bound on IGM enrichment at the time of cloud formation. The metallicity constraint would not apply if Lyα clouds formed *before* protogalactic blastwaves reheated the IGM and avoided mixing with the hotter metal-rich gas as it swept past. Nevertheless, further explorations of metallicity variations in Lyα clouds might provide very useful constraints on the star-formation history of the universe.

5.3. Porosity

Blastwaves initiated after $z = 7$ can fill the IGM by $z = 4$, while still satisfying the above constraints on microwave background distortion and metallicity, as long as the typical explosion size is relatively small. Blastwaves of characteristic energy scale E_0 stemming from star formation at z_1 have a comoving number density $\hat{n}_b = (6.3 \times 10^{-2}\,{\rm Mpc}^{-3})\Omega_* f_{\rm esc} E_{61}$. Multiplying this number density by the typical blastwave volume gives a porosity parameter

$$Q = 111\,\Omega_* f_{\rm esc} E_{61}^{-2/5} h_{50}^{-2/5} \Omega_{\rm IGM}^{-3/5} (1+z_1)^{-3/5} \eta^3 \tag{5-6}$$

analogous to the porosity parameter for supernova remnants in the Galactic interstellar medium (Cox & Smith 1974). Blastwave sources distributed randomly in space shock a fraction $\sim 1 - e^{-Q}$ of the total IGM volume. Shocks from clustered sources merge early, increasing the effective E_0 and lowering the porosity, so Q can be considered an upper limit on the true porosity. Writing Q in terms of the typical blastwave shock velocity v_s yields a particularly illuminating expression:

$$Q = \left(\frac{f_{\rm esc}\Omega_*}{\Omega_{\rm IGM}}\right) \left(\frac{v_s}{790\,{\rm km\,s^{-1}}}\right)^{-2} x^2 \quad , \tag{5-7}$$

where $x = (1+z)/(1+z_1)$. The initial energy input decays adiabatically ($\propto x^2$), and Q approaches unity when this energy has been distributed evenly throughout the IGM. The Comptonization limit on $f_{\rm esc}\Omega_*$ at $z_1 = 7$ permits $Q > 1$ when $v_s < (180\,{\rm km\,s^{-1}})\Omega_{\rm IGM}^{-1/2} h_{50}^{-3/2} x$. The more stringent metallicity limit permits $Q > 1$ when $v_s < (79\,{\rm km\,s^{-1}})x$.

More generally, let Z_{-2} be the IGM metallicity in units of 10^{-2} times the solar metallicity. Spreading the blastwave energy throughout the IGM gives an average IGM temperature $\sim (2 \times 10^5\,\mathrm{K}) Z_{-2} x^2$, if there are no ionization or radiative losses. Requiring $Q > 1$ at $z = 4$ for $z_1 = 7$ in a flat universe then implies $E_0 < (4 \times 10^{57}\,\mathrm{erg}) Q^{-5/2} Z_{-2}^{5/2} h_{50}^{-1} \Omega_{\mathrm{IGM}}$ and $\hat{n}_b > (1.6\,\mathrm{Mpc}^{-3}) h_{50}^3 Z_{-2}^{-3/2}$. This density is much larger than the number density of L_* galaxies and is comparable to the number density of Lyα clouds (§ 6.1). Figures 7 and 8 illustrate these constraints graphically for $\Omega_{\mathrm{IGM}} = 0.01$ and 0.03. The enrichment levels of Lyα clouds thus suggest that the metals they contain originated in relatively small-scale starbursts close to the clouds themselves or in individual population 3 supernovae rather than in enormous protogalactic starbursts.

Quasar blastwaves do not necessarily enrich the IGM with metals, thus they are not bound by the metallicity limit. The Comptonization limit, however, still applies. Because the number density of quasars is low, the energy scale of their blastwaves must be high, if these blastwaves are to fill the universe quickly. The energy density needed for quasar blastwaves to give $Q > 1$ by $z \sim 4$ violates the COBE limits on y-distortion (Voit 1994; see also Figures 7 and 8). Apparently, quasars are too rare to shock-heat the entire IGM before Lyα clouds appear.

6. Blastwaves and Lyα Clouds

Although we have been assuming the IGM is homogeneous, intergalactic space is obviously inhomogeneous. The IGM is filled with clouds responsible for the numerous Lyα absorption lines, known collectively as the Lyα forest, that litter the spectra of high-redshift quasars. The Lyα clouds remain puzzling. Many authors have speculated that these clouds might be linked somehow to cosmological blastwaves. Some have suggested that the absorption lines come from the intergalactic shock fronts themselves (e.g. Chernomordik & Ozernoy 1983). They could also be condensed fragments of primordial blastwaves, now pressure-confined by the IGM (e.g. Ostriker & Cowie 1981; Ikeuchi & Ostriker 1986; Vishniac & Bust 1987), gas that has settled into shallow mini-halos of dark matter (Rees 1986; Bond, Szalay, & Silk 1988), gas collecting at caustics in the dark-matter velocity field (McGill 1990), or pancakes of shocked gas where that velocity field converges (Cen *et al.* 1994). This section explores whether cosmological blastwaves produce observable Lyα absorption lines and examines how these shocks interact with preexisting intergalactic clouds. We find that the postshock H I column densities ($N_{\mathrm{H\,I}}$) in the ambient IGM are much smaller than those of intergalactic Lyα clouds, but blastwaves that interact with preexisting clouds can amplify the Lyα equivalent widths of these clouds significantly.

6.1. Lyα Cloud Characteristics

The joint distribution function describing the number of Lyα clouds $\mathcal{N}$ per redshift interval per column density interval can be written

$$\frac{\partial^2 \mathcal{N}}{\partial N_{\rm H\,I}\,\partial z} = \mathcal{N}_0 N_{14}^{-\beta}(1+z)^{\gamma} \quad , \tag{6-1}$$

where $N_{14} = N_{\rm H\,I}/10^{14}\,{\rm cm}^{-2}$. Marginally opaque clouds ($N_{14} \sim 1$) absorb most of the photons when $1 < \beta < 2$. For this reason, clouds with $N_{\rm H\,I} \sim 10^{14}\,{\rm cm}^{-2}$ are considered typical, even though a power law distribution of column densities fits the data. Press & Rybicki (1993) find $\mathcal{N}_0 \approx 2.6$ and $\beta = 1.43 \pm 0.04$ in a column density range at least as large as $10^{13}\,{\rm cm}^{-2} \lesssim N_{\rm H\,I} \lesssim 10^{16}\,{\rm cm}^{-2}$ for $\gamma = 2.46$ at redshifts $2.5 \lesssim z \lesssim 4$ (Press, Rybicki, & Schneider 1993).[3] The average comoving distance between clouds with $N_{\rm H\,I} > 10^{14}\,{\rm cm}^{-2}$ is then $\sim (7\,{\rm Mpc})[(1+2.5\Omega_0)/3.5]^{-1/2}h_{50}^{-1}$ at $z = 2.5$ and $\sim (1.7\,{\rm Mpc})[(1+4\Omega_0)/5]^{-1/2}h_{50}^{-1}$ at $z = 4$.

Near the redshift of the background quasar, the number density of Lyα absorption lines decreases (Weymann, Carswell, & Smith 1981; Murdoch *et al.* 1986). This "proximity effect" presumably occurs where the ionizing radiation field of the quasar overwhelms the ambient ionizing field. The mean intensity of ionizing radiation at $z \approx 3$ inferred from the proximity effect is $(10^{-21}\,{\rm erg\,cm^{-2}\,s^{-1}\,Hz^{-1}\,ster^{-1}})J_{21}$, where $J_{21} \sim 1 - 3$ (Bajtlik, Duncan, & Ostriker 1988; Bechtold 1994). In photoionization equilibrium, the fractional abundance of atomic hydrogen in an intergalactic cloud is

$$f_{\rm H^0} \approx 2.8 \times 10^{-7}\,(1+z)^3\,D_{\rm cl}\Omega_{\rm IGM}h_{50}^2 J_{21}^{-1}T_4^{-0.8} \quad , \tag{6-2}$$

where $D_{\rm cl}$ is the ratio of the cloud density to the IGM density and T_4 is the cloud temperature in units of 10^4 K, giving a total column density for a typical cloud of

$$N_{\rm H} = (3.6 \times 10^{20}\,{\rm cm}^{-2})\,(1+z)^{-3}\,N_{14}D_{\rm cl}^{-1}\Omega_{\rm IGM}^{-1}h_{50}^{-2}T_4^{0.8}J_{21} \quad . \tag{6-3}$$

Recent observations of the quasar pair Q1343+2640A, B, indicate that the transverse cloud radius $r_{\rm cl} = (200\,{\rm kpc})h_{50}^{-1}r_{200}$ for clouds with $N_{14} \sim 1$ lies in the range $80\,h_{50}^{-1}\,{\rm kpc} < r_{\rm cl} < 560\,h_{50}^{-1}\,{\rm kpc}$ at $z \approx 1.8$ (Bechtold *et al.* 1994; see also Dinshaw *et al.* 1994). This result implies

$$D_{\rm cl} \sim 0.8\,N_{14}^{1/2}\Omega_{\rm IGM}^{-1}h_{50}^{-3/2}T_4^{0.4}J_{21}^{1/2}r_{200}^{-1/2} \tag{6-4}$$

$$N_{\rm H} \sim (2 \times 10^{19}\,{\rm cm}^{-2})N_{14}^{1/2}h_{50}^{-1/2}T_4^{0.4}J_{21}^{1/2}r_{200}^{1/2} \tag{6-5}$$

at $z \sim 2$, if the clouds are roughly spherical. Sheetlike clouds would have a larger $D_{\rm cl}$ and smaller $N_{\rm H}$. Assuming spherical clouds, Bechtold *et al.* (1994) derive a comoving number density $\sim (2\,{\rm Mpc}^{-3})h_{50}^3 r_{200}^{-2}$ for clouds of $N_{14} \sim 1$ at $z \sim 2$. Perhaps coincidentally, this density is similar to the comoving number density of blastwave sources needed to enrich the entire IGM to 10^{-2} times solar by this redshift (§ 5.3).

---

[3]The redshift evolution parameter γ is still not well constrained; current values range from 1.89 (Bechtold 1994) to 2.75 (Lu, Wolfe, & Turnshek 1991).

6.2. IGM Ionization Constraints

We see a Lyα forest because the spaces between Lyα clouds are either gas free or highly ionized. Gunn & Peterson (1965) inferred $f_0\Omega_{\rm IGM} \equiv \Omega_{\rm H\ I} < 6 \times 10^{-7}\, h_{50}^{-1}$ from the lack of continuous absorption at $z \approx 2$. Observations at the wavelength of He II Lyα (304 Å) toward a quasar at $z = 3.286$ show that intergalactic He II absorbing gas fills velocity space at $z \sim 4$ (Jakobsen *et al.* 1994). Although this observation appears to confirm that the IGM has a spatially continuous component, the cumulative He II absorption of many very thin velocity-broadened Lyα clouds ($N_{\rm H\,I} \gtrsim 10^{-12}\,{\rm cm}^{-2}$) could also produce the observed signal (Madau & Meiksin 1994). Current limits on $\Omega_{\rm H\,I} = 10^{-8}\,\Omega_8$ in a spatially continuous component are $\Omega_8 < 4.3\, h_{50}^{-1}$ at $z \approx 2.5$ (Steidel & Sargent 1987) and $\Omega_8 < 2.5\, h_{50}^{-1}$ at $z \approx 4$ (Webb *et al.* 1992; Giallongo *et al.* 1994). Photoionization equilibrium thus implies $\Omega_{\rm IGM} < 0.016\, h_{50}^{-1} T_4^{0.4} J_{21}^{1/2} \Omega_8^{1/2}$ at $z = 4.1$.

Alternatively, the IGM could be collisionally ionized by early supernovae (Tegmark, Silk, & Evrard 1993), but if the metallicity of the IGM is similar to that of Lyα clouds, photoionization is likely to be more important. The mean temperature in an IGM heated by supernova-driven blastwaves is $\lesssim (2 \times 10^5\,{\rm K}) Z_{-2}$ (§ 5.3), and pure collisional ionization at $2 \times 10^5\,{\rm K}$ requires $\Omega_{\rm IGM} < 3.6 \times 10^{-3}\,\Omega_8$ for Lyα to be transparent at the observed levels, a condition more stringent than the photoionization condition. An elevated temperature does, however, reduce the IGM recombination rate, easing the photoionization constraint on $\Omega_{\rm IGM}$ (e.g. Shapiro 1995).

6.3. Shocked Shells as Lyα Clouds

In principle, a sufficiently large compression of the IGM in a shock along the line of sight to a quasar could produce an observable Lyα feature (Ozernoy & Chernomordik 1978; Chernomordik & Ozernoy 1983). This can happen if $\Omega_{\rm IGM} \sim 1$, but since $\Omega_{\rm IGM} \lesssim 10^{-2}$, as the ionization constraints indicate, the H I column densities of cosmological blastwaves in the ambient IGM are much smaller than typical Lyα-cloud column densities ($N_{\rm H\,I} \sim 10^{14}\,{\rm cm}^{-2}$). The total hydrogen column density within a cosmological shock is $N_{\rm asy}(1+z)^2\eta$, where

$$N_{\rm asy} = (1.6 \times 10^{19}\,{\rm cm}^{-2}) E_{61}^{1/5} h_{50}^{6/5} \Omega_{\rm IGM}^{4/5} (1+z_1)^{1/5} \quad . \tag{6-6}$$

Figure 9 shows how the shocked column density evolves for various blastwave parameters and $\Omega_{\rm IGM} = 0.01$. Behind a strong adiabatic cosmological shock, $D_{\rm cl} = 4$ until $t \sim \Omega_{\rm IGM}^{-3/2} t_1$ (§ 2.5.3). Initially, electron collisions keep the postshock gas highly ionized. As the shock slows, photoionization maintains a relatively high ionization level. If collisional ionization can be neglected, the neutral column behind the shock is

$$N_{\rm H\,I} \approx (1.7 \times 10^{13}\,{\rm cm}^{-2})(1+z)^5 E_{61}^{1/5} h_{50}^{16/5} \Omega_{\rm IGM}^{9/5} T_4^{-0.8} J_{21}^{-1} (1+z_1)^{1/5} \eta \quad . \tag{6-7}$$

Figure 10 illustrates $N_{\rm H\,I}(z)$ for a range of blastwave parameters and $\Omega_{\rm IGM} = 0.01$. The lines indicating $N_{\rm H\,I}$ are dashed when collisional ionization exceeds photoionization and solid when photoionization exceeds collisional ionization. Low-energy blastwaves produce larger neutral columns because they have smaller postshock temperatures ($T_4 \propto E_{61}^{2/5}$). Unless $\Omega_{\rm IGM} \sim 1$, Lyα absorption in adiabatic blastwaves is much weaker than in Lyα clouds.

Cooling can potentially magnify the postshock density, boosting the neutral column in the blastwave, but the compression ratios of radiative cosmological shocks in the ambient IGM are unlikely to be very large. At $z \sim 2$, shocks with $E_0 \lesssim 10^{57}\,{\rm erg}$ can cool in a Hubble time in a medium with $\Omega_{\rm IGM} \lesssim 0.03$ (Figure 2). The requisite shock velocities are $\lesssim 40 - 50\,{\rm km\,s}^{-1}$, not much larger than the velocity dispersions of Lyα clouds. The widths of intergalactic Lyα lines, if thermal, imply temperatures $\sim 3 \times 10^4\,{\rm K}$, consistent with photoelectric heating by quasars. If the intercloud gas is at least as hot, radiative IGM shocks have Mach numbers $\lesssim 3$, too weak to produce $N_{\rm HI} \sim 10^{14}\,{\rm cm}^{-2}$ when $\Omega_{\rm IGM} \lesssim 0.03$. Allowing $\Omega_{\rm IGM} \sim 0.1$ requires an IGM temperature $\gtrsim 10^6\,{\rm K}$ for Lyα to remain transparent. Even in this denser environment, the Mach numbers of radiative shocks, with velocities $< 200\,{\rm km\,s}^{-1}$ (§ 2.2), would still be too low to increase $D_{\rm cl}$ sufficiently.

6.4. Shock-Cloud Interactions

Since blastwaves in a low-density IGM have insignificant neutral columns, Lyα clouds form through some other means. The porosity and metallicity constraints discussed in § 5 argue

against pressure confinement of Lyα clouds. Mechanisms in which interstellar gas collects in "minihaloes" of dark matter (e.g. Rees 1986) or converges at caustics in the large-scale velocity field (e.g. McGill 1990, Cen *et al.* 1994) appear to be more likely. Fluctuations in the spatial distribution of collisionless matter certainly alter the density field of the IGM, which we have so far idealized as uniform. Real intergalactic shocks propagate through an inhomogeneous medium; hence, the solutions derived above become accurate only after the shock radius exceeds the length scales of non-linear density perturbations. The remainder of this section briefly examines how interactions between cosmological blastwaves and density inhomogeneities proceed and suggests that intergalactic blastwaves might amplify the neutral column densities of preexisting Lyα clouds.

Shock propagation into an inhomogeneous interstellar medium has been analyzed extensively (McKee & Cowie 1975; Woodward 1976; Nittman, Falle, & Gaskell 1982; Stone & Norman 1992; Klein, McKee, & Colella 1994). When a shock of velocity v_s encounters a cloud $D_{\rm cl}$ times denser than the ambient medium, it drives a shock of velocity $D_{\rm cl}^{-1/2} v_s$ into the cloud. In a cloud-crushing time ($t_{\rm cc} \sim D_{\rm cl}^{1/2} r_{\rm cl} v_{\rm cl}$), the internal shock crosses the cloud. Detailed numerical simulations show that the vorticity generated in the cloud-shock collision shreds the cloud in a few cloud-crushing times (Nittman *et al.* 1982; Stone & Norman 1992; Klein *et al.* 1994). If Lyα clouds are indeed several hundred kpc in size, the cloud shredding time approaches a Hubble time for v_s less than a few times $10^2\,{\rm km\,s^{-1}}$. Since the postshock cooling time in the cloud is smaller than the ambient cooling time by a factor $\sim D_{\rm cl}^2$, such long-lived clouds, or fragments thereof, might collapse to much higher density before vorticity destroys the cloud. The resulting $N_{\rm H\,I}$ would then increase by a factor $\sim v_s^2/v_{th}^2$, where $v_{th} \sim 30\,{\rm km\,s^{-1}}$ is the thermal velocity dispersion of the photoionized cloud after it has cooled to its equilibrium temperature. Such a shock would impart a velocity $D_{\rm cl}^{-1/2} v_s$ to the cloud, perhaps carrying it out of its potential well. Figure 11 illustrates how large $D_{\rm cl}$ must be for shocked clouds to cool within a Hubble time. In the example shown, shocks of $E_0 = 10^{57}$, 10^{59}, and $10^{61}\,{\rm erg}$ begin propagating at $z_1 = 4$ in an $\Omega = 1$, $h_{50} = 1$ universe with $\Omega_{\rm IGM} = 0.01$. Clouds with $D_{\rm cl} = 6$ at $z \gtrsim 2$, for instance, can cool after encountering shocks of $v_s \lesssim 200\,{\rm km\,s^{-1}}$.

Computing in detail how cosmological blastwaves interact with developing gaseous structures in the IGM is beyond the scope of this paper; however, the cooling times estimated here indicate that blastwaves could dramatically alter the observable characteristics of preexisting Lyα clouds. In essence, shocked clouds are pressure-confined, but the pressurizing medium does not pervade the universe. Instead, the pressurized regions are the interiors of individual blastwaves. Clouds near blastwave sources would then have systematically higher neutral column densities than clouds in the ambient IGM.

7. Summary

This paper has investigated the behavior of protogalactic and quasar-driven blastwaves in an expanding universe with $\Omega_{\rm IGM} \ll \Omega_0$. It presents a new analytical solution for adiabatic blastwaves that applies until $t \sim t_1 \Omega_{\rm IGM}^{-3/2}$, when self-gravity starts to compress the postshock gas into a thin shell. Although two different timescales (t and t_1) enter into the problem, a self-similar solution still exists. The similarity of the universe's expansion allows us to define another time coordinate ($\hat{t}$) in which the Sedov-Taylor solution satisfies an appropriately transformed set of fluid equations if $\gamma = 5/3$. Cosmological blastwaves thus begin as Sedov-Taylor blastwaves and approach a constant comoving radius as t grows large. While $t \ll t_1 \Omega_{\rm IGM}^{-3/2}$, the gas density immediately behind the shock remains equal to four times the ambient density, so cosmological shocks do not cool until they are moving quite slowly.

Applying this solution to protogalactic starbursts and quasars shows that small-scale explosions ($\lesssim 10^{57}$erg) are probably more important than large-scale explosions ($\gtrsim 10^{58}\,$erg) in determining the state of the IGM and its Lyα clouds. Large-scale explosions are quite inefficient at ionizing the IGM. Cosmological effects rob most of the energy from large-scale blastwaves before these shocks slow to speeds that ionize efficiently ($\lesssim 100\,{\rm km\,s^{-1}}$). In addition, since the comoving volume per unit energy of a blastwave is $\propto E_0^{-2/5}$, small-scale explosions can fill the IGM much more easily. Quasar-driven blastwaves are too rare to fill the IGM by $z \sim 4$ without violating the y-parameter limit from COBE. Large-scale protogalactic blastwaves that filled the universe by such an early time would raise the mean metallicity of the IGM well above the values observed in Lyα clouds at $z \sim 2 - 3$.

Contrary to some suggestions that Lyα clouds might be shells of gas shocked by cosmological blastwaves, the solution derived here shows that the postshock gas never becomes dense enough to produce $N_{\rm H\,I} \gtrsim 10^{13}\,{\rm cm^{-3}}$ when $\Omega_{\rm IGM} \lesssim 0.03$. Even if the blastwave has slowed enough to cool, the compression of the ambient IGM is still too small to raise $N_{\rm H\,I}$ to the levels observed in Lyα clouds. Blasts that pass through overdense regions of the IGM, such as preexisting Lyα clouds, might still produce observable signatures. Compression and cooling can dramatically amplify the neutral fraction in a shocked cloud, so clouds engulfed by blastwaves could have systematically higher values of $N_{\rm H\,I}$. This effect would increase the probability of finding clouds near blastwave sources.

During the development of this paper, conversations with Steve Balbus, Megan Donahue, Mike Fall, Piero Madau, and Sterl Phinney were particularly helpful. The author gratefully acknowledges the hospitality of the Virginia Institute for Theoretical Astrophysics during the early stages of this project. The work presented here was supported by NASA through grant number HF-1054.01-93 from the Space Telescope Science Institute, which is operated by the Association of Universities for Research in Astronomy, Inc., under NASA contract NAS5-26555.

REFERENCES

Bajtlik, S., Duncan, R. C., & Ostriker, J. P. 1988, ApJ, 327, 570

Bechtold, J. 1994, ApJS, 91, 1

Bechtold, J., Crotts, A. P. S., Duncan, R. C., & Fang, Y. 1994, ApJ, 437, L83

Bertschinger, E. J. 1983, ApJ, 268, 17

Bertschinger, E. J. 1985, ApJS, 58, 1

Bertschinger, E. J. 1986, ApJ, 304, 154

Bond, J. R. 1993, in The Environment and Evolution of Galaxies, ed. J. M. Shull & H. A. Thronson (Dordrecht: Kluwer), 3

Bond, J. R., Szalay, A. S., & Silk, J. 1988, ApJ, 324, 627

Boyle, B. J. 1993, in The Environment and Evolution of Galaxies, ed. J. M. Shull & H. A. Thronson (Dordrecht: Kluwer), 433

Cen, R. Y., & Ostriker, J. P. 1993, ApJ, 417, 404

Cen, R. Y., Miralda-Escude, J., Ostriker, J. P., & Rauch, M. 1994, ApJ, 437, L9

Chernomordik, V. V., & Ozernoy, L. M. 1983, Nature, 303, 153

Cowie, L. L., Songaila, A., Kim, T.-S., & Hu, E. M. 1995, AJ, 109, 1522

Cox, D. P., & Smith, B. W. 1974, ApJ, 189, L105

Dinshaw, N., Impey, C. D., Foltz, C. B., Weymann, R. J., Chaffee, F. H. 1994, ApJ, 437, L87

Donahue, M., & Shull, J. M. 1987, ApJ, 323, L13

Draine, B. T., & McKee C. F. 1993, ARA&A, 31, 373

Field, G. B. 1995, in The Physics of the Interstellar Medium and the Intergalactic Medium, ed. A. Ferrara, C. F. McKee, C. Heiles, & P. R. Shapiro, (San Francisco: Astronomical Society of the Pacific), p. 1

Giallongo, E., D'Odorico, S., Fontana, A., McMahon, R. G., Savaglio, S., Cristiani, S., Molaro, P., & Trevese, D. 1994, ApJ, 425, L1

Grun, J., Stamper, J., Manka, C., Resnik, J., Burris, R., Crawford, J., & Ripin, B. H. 1991, Phys. Rev. Lett., 66, 2738

Gunn, J. E., & Peterson, B. A. 1965, ApJ, 142, 1633

Heckman, T. M., Lehnert, M. D., & Armus L. 1993, in The Environment and Evolution of Galaxies, ed. J. M. Shull & H. A. Thronson (Dordrecht: Kluwer), 433

Hogan, C. J. 1984, ApJ, 284, L1

Ikeuchi, S., Tomisaka, K., & Ostriker, J. P. 1981, ApJ, 265, 583

Ikeuchi, S., Tomisaka, K., & Ostriker, J. P. 1983, ApJ, 265, 583

Ikeuchi, S. & Ostriker, J. P. 1986, ApJ, 301, 522

Jakobsen, P., Boksenberg, A., Deharveng, J. M., Greenfield, P., Jedrzejewski, R., & Paresce, F. 1994, Nature, 370, 35

Klein, R. I., McKee, C. F., & Colella, P. 1994, ApJ, 420, 213

Kronberg, P. P. 1994, Rep. Prog. Phys., 57, 325

Kulsrud, R. M., & Anderson, S. W. 1992, ApJ, 396, 606

Leitherer, C., & Heckman, T. M. 1995, ApJS, in press

Lu, L. 1991, ApJ, 379, 99

Lu, L., Wolfe, A. M., & Turnshek, D. A. 1991, ApJ, 367, 19

Mac Low, M.-M. & Norman, M. L. 1994, ApJ, 407, 207

Madau, P., & Meiksin, A. 1991, ApJ, 374, 6

Madau, P., & Meiksin, A. 1991, ApJ, 433, L53

Madau, P., & Shull, J. M. 1995, ApJ, in press

Mather, J. C. *et al.* 1994, ApJ, 420, 439

McGill, C. 1990, MNRAS, 242, 544

McKee, C. F., & Cowie, L. L. 1975, ApJ, 195, 715

Mishustin, I. N., & Ruzmaikin, A. A. 1972, Soviet Phys. – JETP, 34, 233

Murdoch, H. S., Hunstead, R. W., Pettini, M., & Blades, J. C. 1986, ApJ, 309, 19

Navarro, J. F., & White, S. D. M. 1993, ApJ, 267, 401

Nittman, J. Falle, S., & Gaskell, P. 1982, MNRAS, 201, 833

Ostriker, J. P., & Cowie, L. L. 1981, ApJ, 243, L127

Ostriker, J. P., & McKee, C. F. 1988, Rev. Mod. Phys., 60, 1

Ozernoy, L. M., & Chernomordik, V. V. 1978, Sov. Ast., 22, 141

Parker, E. N. 1979, Cosmical Magnetic Fields (Oxford: Clarendon Press)

Press, W. H., & Rybicki, G. B. 1993, ApJ, 418, 585

Press, W. H., Rybicki, G. B., & Schneider, D. P. 1993, ApJ, 414, 64

Ratra, B. 1992, ApJ, 391, L1

Rees, M. J. 1986, MNRAS, 218, 25P

Schmutzler, T., & Tscharnuter, W. M. 1993, A&A, 273, 318

Schwarz, J., Ostriker, J. P., & Yahil, A. 1975, ApJ, 202, 1

Sedov, L. I. 1959, Similarity and Dimensional Methods in Mechanics (New York: Academic)

Sedov, L. I. 1993, Similarity and Dimensional Methods in Mechanics, 10th Edition (Boca Raton: CRC Press)

Shandarin, S. 1980, Astrofizika, 16, 769

Shapiro, P. R. 1995, in The Physics of the Interstellar Medium and the Intergalactic Medium, ed. A. Ferrara, C. F. McKee, C. Heiles, & P. R. Shapiro, (San Francisco: Astronomical Society of the Pacific), p. 55

Shapiro, P. R., & Giroux, M. L. 1987, ApJ, 321, L107

Shapiro, P. R., Struck-Marcell, C., & Melott, A. L. 1983, ApJ, 275, 413

Spitzer, L. 1962, Physics of Fully Ionized Gases, (New York: Wiley), 2nd ed.

Steidel, C. C., & Sargent, W. L. W. 1987, ApJ, 318, L11

Stone, J. M., & Norman, M. L. 1992, ApJ, 390, L17

Sunyaev, R. A. & Zel'dovich, Ya. B. 1980, ARA&A, 18, 537

Sutherland, R. S., & Dopita, M. A. 1993, ApJS, 88, 253

Tegmark, M., Silk, J., & Evrard, A. 1993, ApJ, 417, 54

Tidman, D. A., & Krall, N. A. 1971, Shock Waves in Collisionless Plasmas, (Wiley-Interscience: New York)

Tytler, D. & Fan, X.-M. 1994, ApJ, 424, L87

Vishniac, E. T. 1983, ApJ, 274, 152

Vishniac, E. T., & Bust, G. S. 1987, ApJ, 319, 114

Vishniac, E. T., Ostriker, J. P., & Bertschinger, E. 1985, ApJ, 291, 399

Voit, G. M. 1988, ApJ, 331, 343

Voit, G. M. 1994, ApJ, 432, L19

Voit, G. M., Weymann, R. J., & Korista, K. T. 1993, ApJ, 413, 95

Webb, J. K., Barcons, X., Carswell, R. F., & Parnell, H. C. 1992, MNRAS, 255, 319

Weymann, R. J. 1965, Phys. Fluids, 8, 2112

Weymann, R. J. 1966, ApJ, 145, 560

Weymann, R. J., Carswell, R. F., & Smith, M. G. 1981, ARA&A, 19, 41

Wolfe, A. M., Lanzetta, K. M., & Oren A. L. 1992, ApJ, 388, 17

Woodward, P. R, 1976, ApJ, 207, 484

Yoshioka, S., & Ikeuchi, S. 1987, ApJ, 323, L7

Yoshioka, S., & Ikeuchi, S. 1988, PASJ, 40, 383

This preprint was prepared with the AAS LaTeX macros v3.0.

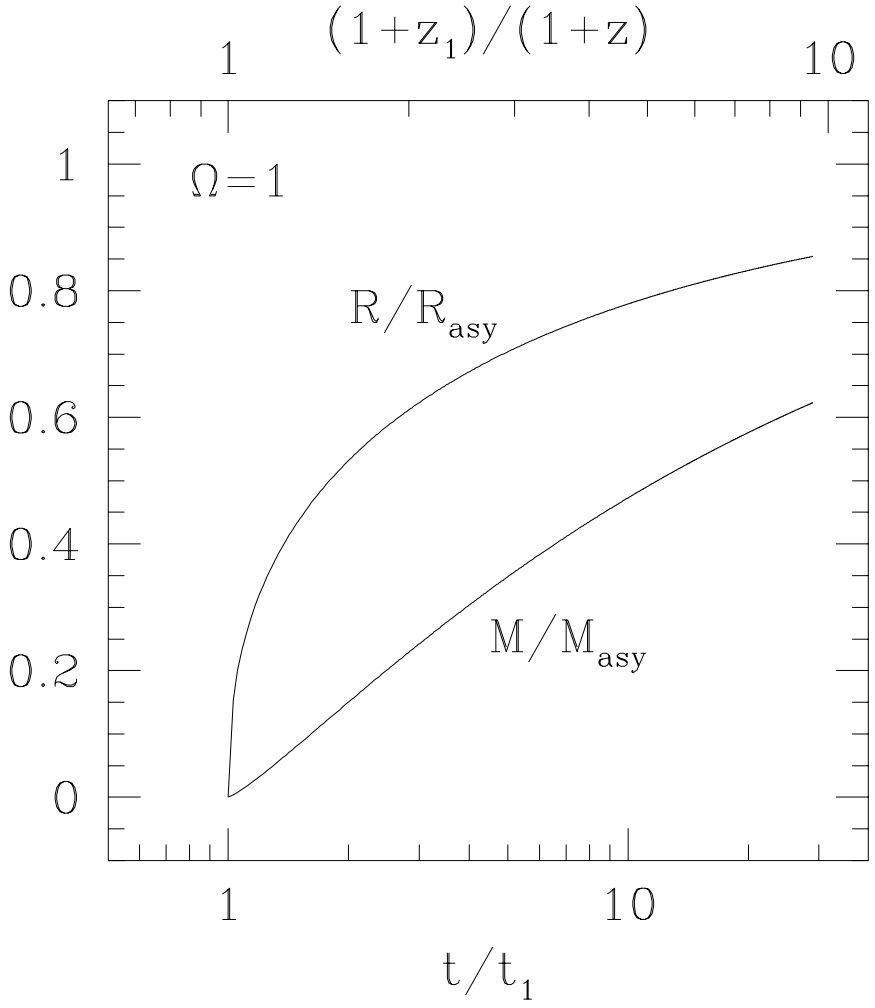

Fig. 1.— Growth of an adiabatic cosmological blastwave when $\Omega_{\rm IGM} \ll \Omega_0 = 1$. This figure illustrates how quickly the radius and mass of an adiabatic cosmological blastwave arising from an intergalactic explosion at cosmic time t_1 approach their asymptotic values. At cosmic time t, the shock radius has reached a fraction $R/R_{\rm asy}$ of its asymptotic comoving value and contains a fraction $M/M_{\rm asy}$ of the mass it will ultimately encompass.

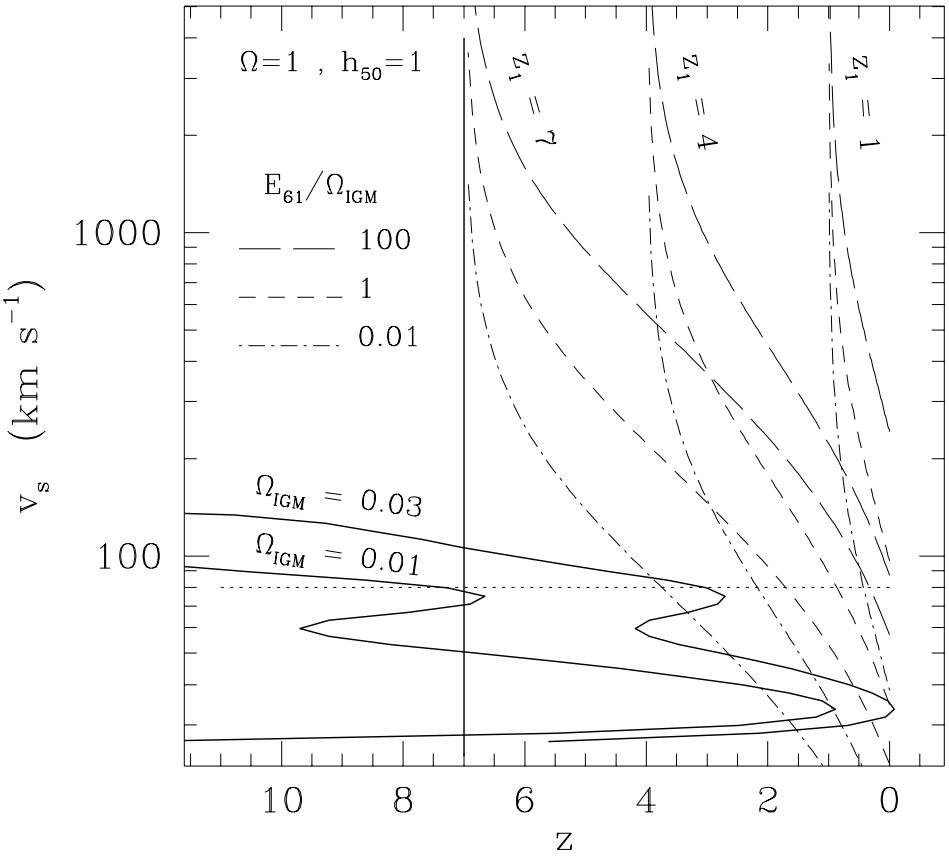

Fig. 2.— Shock velocities of adiabatic cosmological blastwaves. The velocity $v_s(z)$ of the adiabatic shock driven into the IGM when an energy $(10^{61}\ \mathrm{erg})E_{61}$ is introduced at redshift z_1 depends on z_1, Ω, and the value of $E_{61}h_{50}\Omega_{\mathrm{IGM}}^{-1}$. Here we show how v_s varies with z for several values of $E_{61}\Omega_{\mathrm{IGM}}^{-1}$ when $h_{50} = 1$, $\Omega = 1$, and $\Omega_{\mathrm{IGM}} \ll 1$. Curves corresponding to shocks beginning at three different initial redshifts ($z_1 = 1, 4, 7$) are shown. The solid lines indicate where cooling begins to violate the assumption that the shocks are adiabatic. The vertical line at $z = 7$ shows where Compton cooling against the microwave background becomes important, and the two lines across the bottom show where radiative cooling becomes important for $\Omega_{\mathrm{IGM}} = 0.01$ and 0.03, assuming an IGM metallicity of 0.01 times solar (radiative cooling functions from Sutherland & Dopita 1993). The horizontal dashed line shows where ionization losses would become important if the ambient medium were neutral. Since the $v_s(z)$ curves lie primarily above and to the right of the solid lines, cosmological shocks at $z < 7$ are adiabatic for a wide range of parameters.

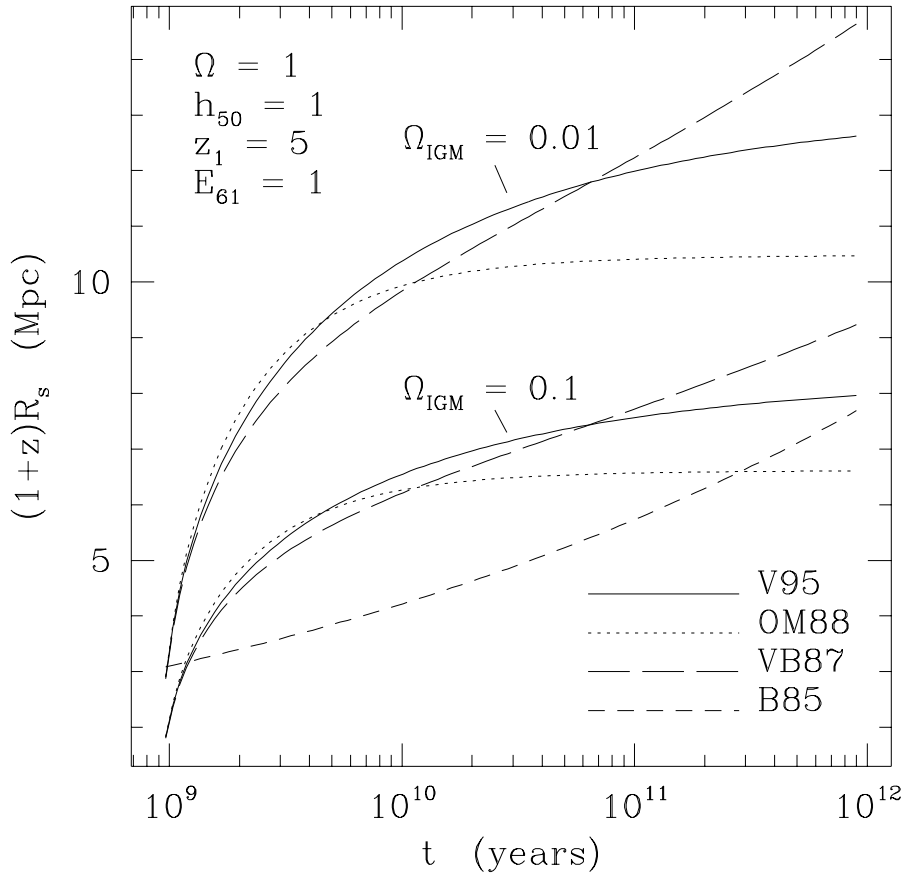

Fig. 3.— Approximate solutions for adiabatic cosmological blastwaves when $\Omega_{\rm IGM} \ll \Omega_0 = 1$. Solid lines (V95) show the exact solutions from § 2.1 for $R_s(t)$ in comoving coordinates, given a 10^{61} erg blastwave starting at $z_1 = 5$ in intergalactic media with $\Omega_{\rm IGM} = 0.1$ and $\Omega_{\rm IGM} = 0.01$. These solutions become invalid when $t \sim t_1 \Omega_{\rm IGM}^{-3/2}$. Dotted lines (OM88) show the approximate solutions derived by Ostriker & McKee (1988) for these same parameters. The long-dashed line (VB87) gives the approximate fit of Vishniac & Bust (1987) to numerical models. The short-dashed line (B85) gives the self-similar solution from Bertschinger (1985), valid when $t \gg t_1 \Omega_{\rm IGM}^{-3/2}$ and the shocked IGM comoves with a collisionless shell that has responded to the blastwave.

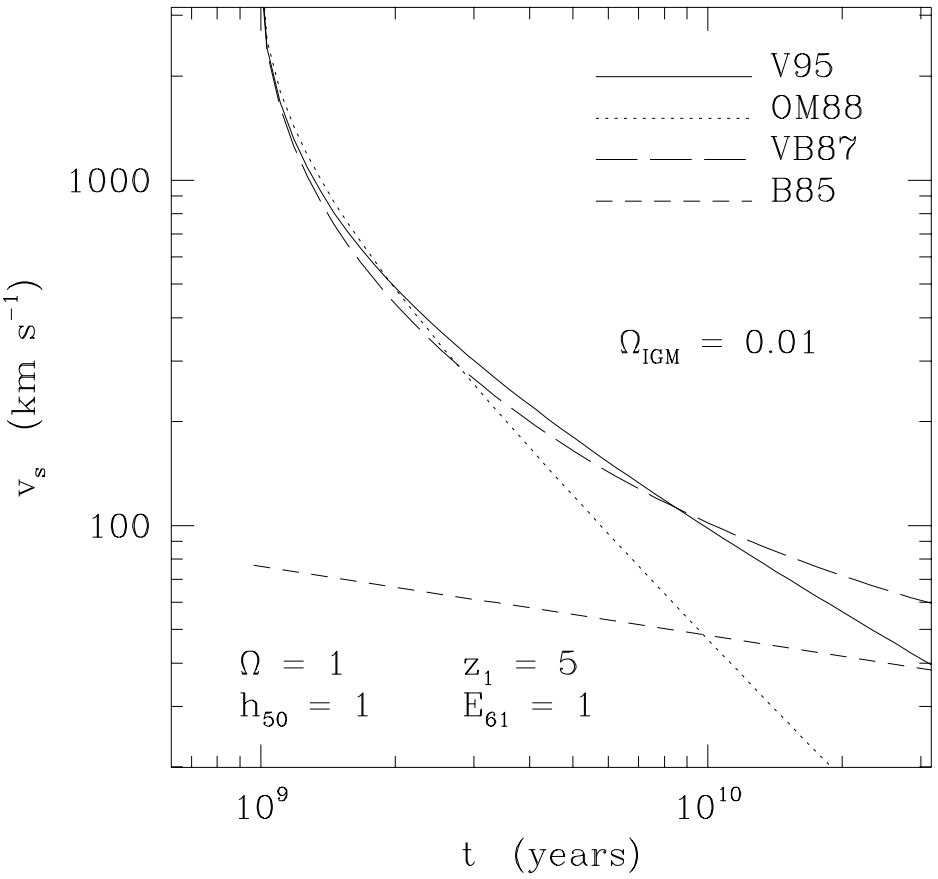

Fig. 4.— Approximate shock velocities. The lines in this figure trace the shock velocities given by the approximate blastwave solutions in Figure 3.

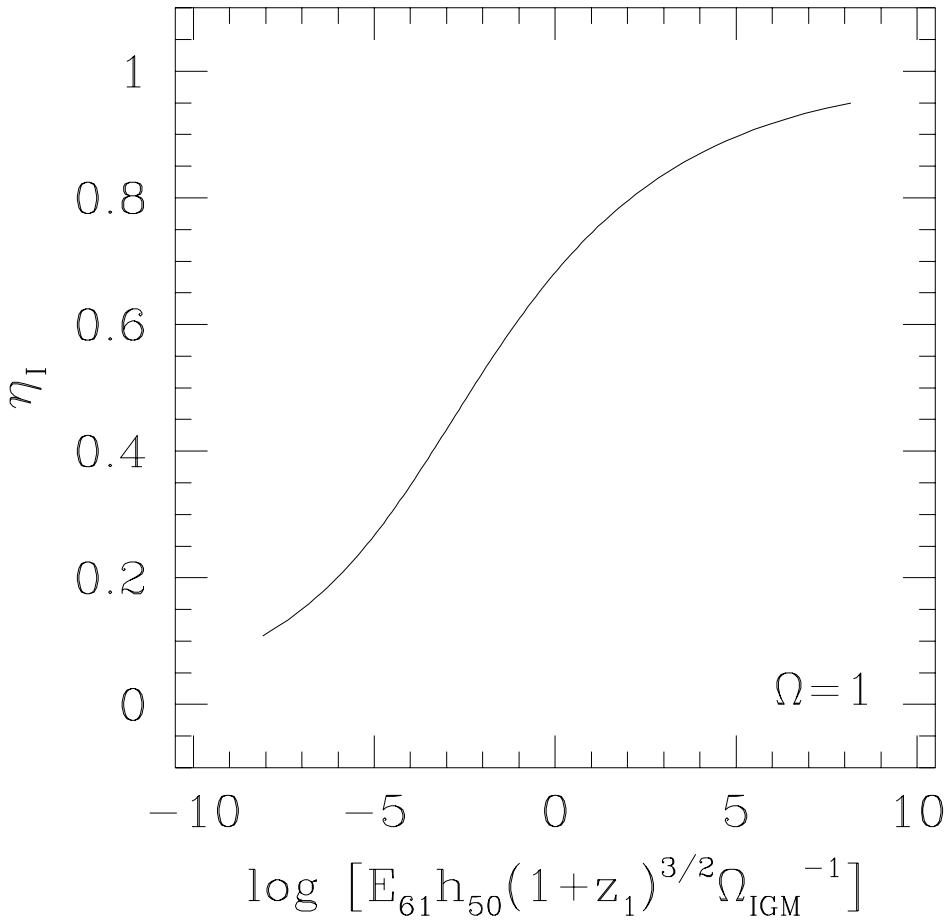

Fig. 5.— Dimensionless comoving radius at which shock ionization becomes ineffective ($\Omega = 1$). The quantity η_I is the value of $\eta \equiv \hat{R}_s/\hat{R}_{\rm asy}$ at which the shock velocity drops below $50\,{\rm km\,s^{-1}}$. Beyond this point, the shock no longer provides enough energy to ionize the incoming hydrogen. When E_{61} is large, η_I is of order unity, and cosmological effects have begun to govern the growth of the blastwave.

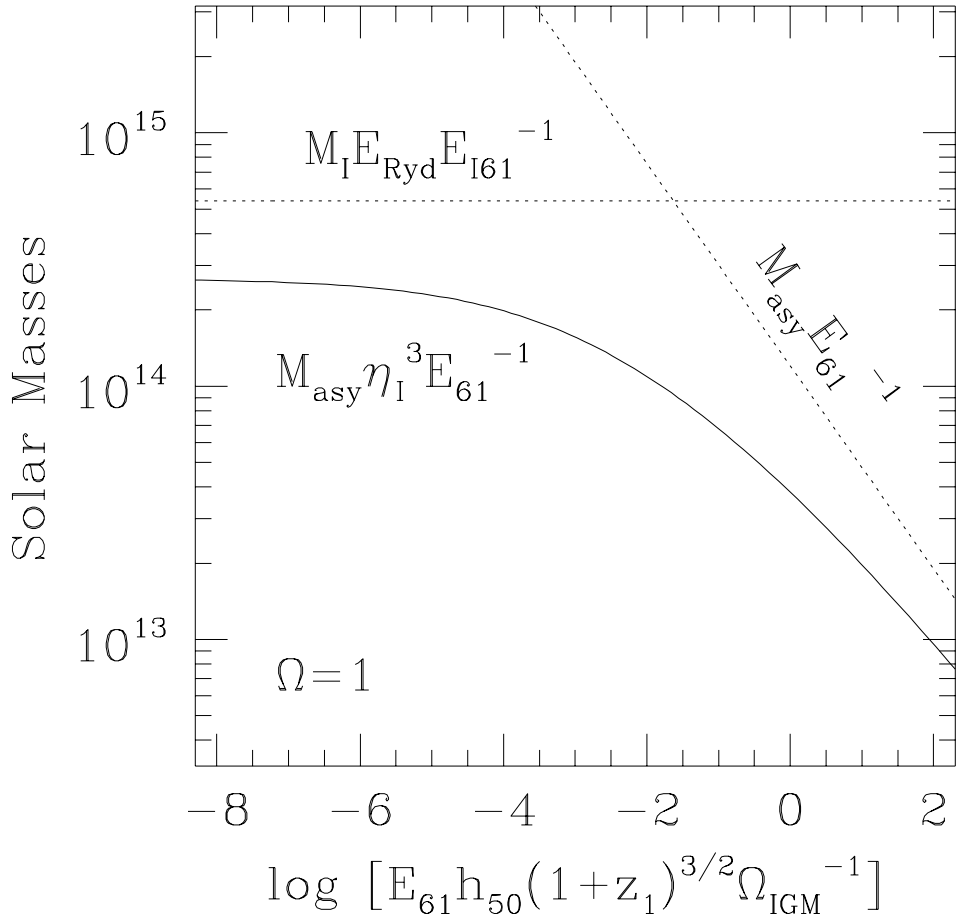

Fig. 6.— Total ionized mass when $\Omega = 1$. The horizontal dotted line gives the total mass (M_I) ionized by $(10^{61}\,\mathrm{erg})E_{I61}$ in ionizing photons with mean energy $(13.6\,\mathrm{eV})E_{\mathrm{Ryd}}$. An adiabatic blastwave initially containing $(10^{61}\,\mathrm{erg})E_{61}$ ultimately encompasses a mass M_{asy}. The diagonal dotted line shows how this asymptotic mass varies with the parameter combination $E_{61}h_{50}(1+z_1)^{3/2}\Omega_{\mathrm{IGM}}^{-1}$ in a flat universe. The solid line gives the amount of mass ($M_{\mathrm{asy}}\eta_I^3$) within an adiabatic blastwave when the shock ceases to ionize the incoming gas efficiently. The maximum amount of collisionally ionized mass per unit input energy drops with increasing energy because high-energy blastwaves transfer most of their energy to the collisonless component before ionization losses become important. Cosmological blastwaves do not ionize the IGM unless their sources emit relatively few ionizing photons into intergalactic space.

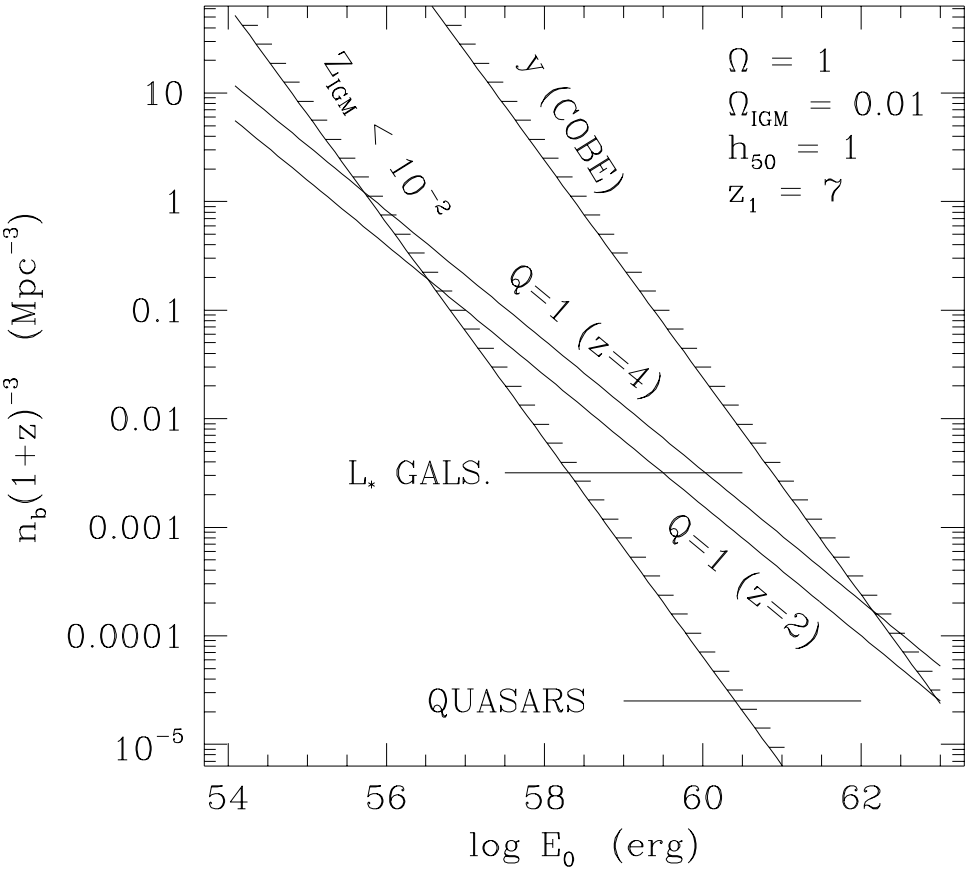

Fig. 7.— Constraints on porosity. COBE limits on the y-distortion of the microwave background constrain the thermal energy density of the IGM at high redshift. The product of the energy per blastwave, E_0, and the comoving number density of blastwave sources, $n_b(1+z)^{-3}$, must therefore lie below the line marked y (COBE), if $\Omega = 1$, $h_{50} = 1$, and $z_1 = 7$. Blastwaves driven into the IGM by multiple supernovae introduce metals along with thermal energy. If the metallicities of Lyα clouds ($\lesssim 10^{-2}$ times solar) are similar to the mean metallicity of the IGM, the energy density injected by supernovae must be significantly lower than the COBE limit. The line marked $Z_{\rm IGM} < 10^{-2}$ indicates the value of $E_0 n_b(1+z)^{-3}$ that would yield an IGM metallicity of 10^{-2} times solar, assuming each supernova produces $1\,M_\odot$ of metals and $\Omega_{\rm IGM} = 0.01$. The lines labeled $Q = 1$ trace the locus of blastwave parameters that give $Q = 1$ at $z = 4$ and $z = 2$ for blastwaves that begin propagating at $z_1 = 7$. (See Fig. 8 caption for additional information.)

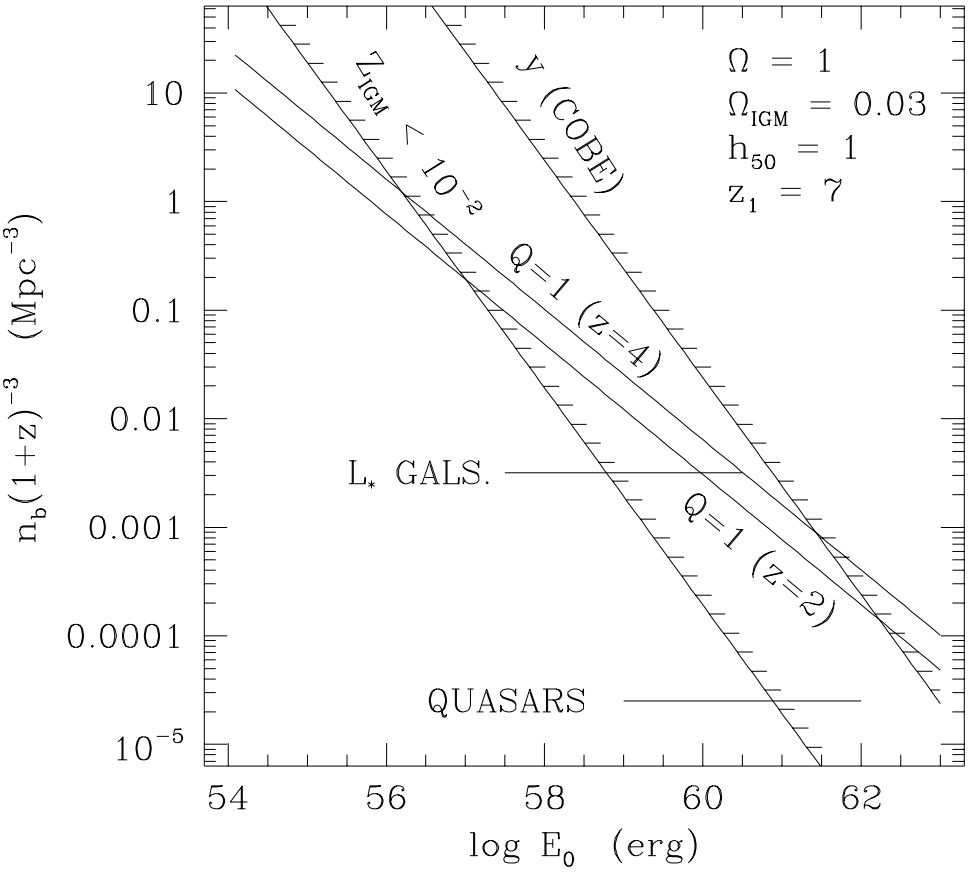

Fig. 8.— Constraints on porosity. Same as Figure 7, except $\Omega_{\rm IGM} = 0.03$. The metallicity constraint allows $Q \gg 1$ at $z > 2$ only if blastwave sources are much more numerous than L_* galaxies and the energy per blastwave is $\ll 10^{57}$ erg. Quasar blastwaves could be metal-free and need not satisfy the metallicity constraint; however, the COBE constraint rules out $Q(z > 2) \gg 1$ in quasar blastwaves if $\Omega_{\rm IGM} \geq 10^{-2}$. The line marked QUASARS indicates the comoving number density of quasars measured at $z = 2$ by Boyle (1993), multiplied by a factor of 10 to account for the quasar duty cycle (quasar lifetime $\sim 10^8$ yr divided by $t \sim 10^9$ yr at $z \sim 5$). Blastwaves driven by objects this uncommon cannot fill the universe by $z > 2$, while still satisfying the COBE constraint, regardless of their energy output.

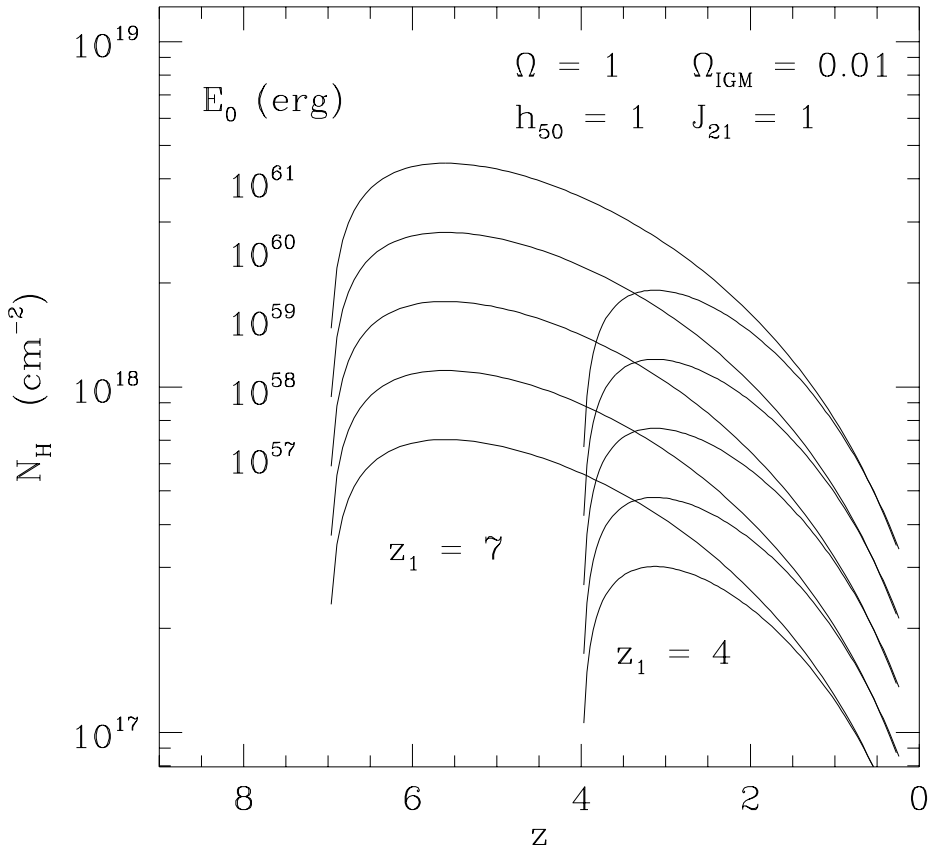

Fig. 9.— Postshock H column density. This figure shows how the column density of hydrogen behind a spherical cosmological shock changes with time in a uniform IGM. The curves indicate $N_{\rm H}$ in blasts beginning at redshifts $z_1 = 4$ and 7 with initial energies in the range $10^{57} - 10^{61}$ erg. We assume $\Omega_{\rm IGM} = 0.01$, $h_{50} = 1$, and $\Omega = 1$. Note $N_{\rm H} \propto \Omega_{\rm IGM}^{4/5} h_{50}^{6/5}$. At first, $N_{\rm H}$ grows. Later, as the shock begins to merge with the Hubble flow, $N_{\rm H}$ drops.

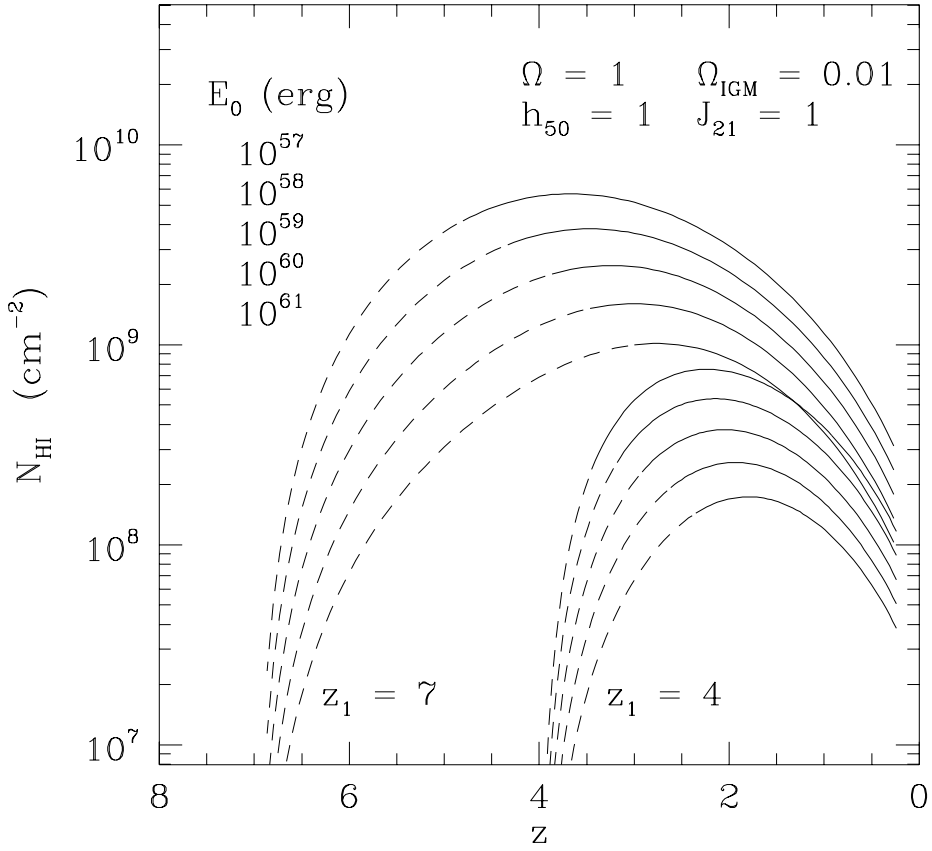

Fig. 10.— Postshock H I column density. This figure gives the neutral postshock column densities for the same blastwaves described in Figure 9. The shocks are presumed to be adiabatic (not true for $E_0 \sim 10^{57}$ erg at $z < 1.5$) and strong enough for the postshock density to be four times the IGM density. Collisional ionization governs postshock ionization balance at early times, indicated by the dashed lines. Later, photoionization ($J_{21} = 1$) overtakes collisional ionization. The transition from dashed to solid lines occurs where photoionization and collisional ionization are equally important. Low energy blastwaves have higher $N_{\rm H\,I}$ because their postshock temperatures are lower, allowing recombination to act more rapidly. Note $N_{\rm H\,I} \propto \Omega_{\rm IGM}^{9/5} h_{50}^{16/5}$.

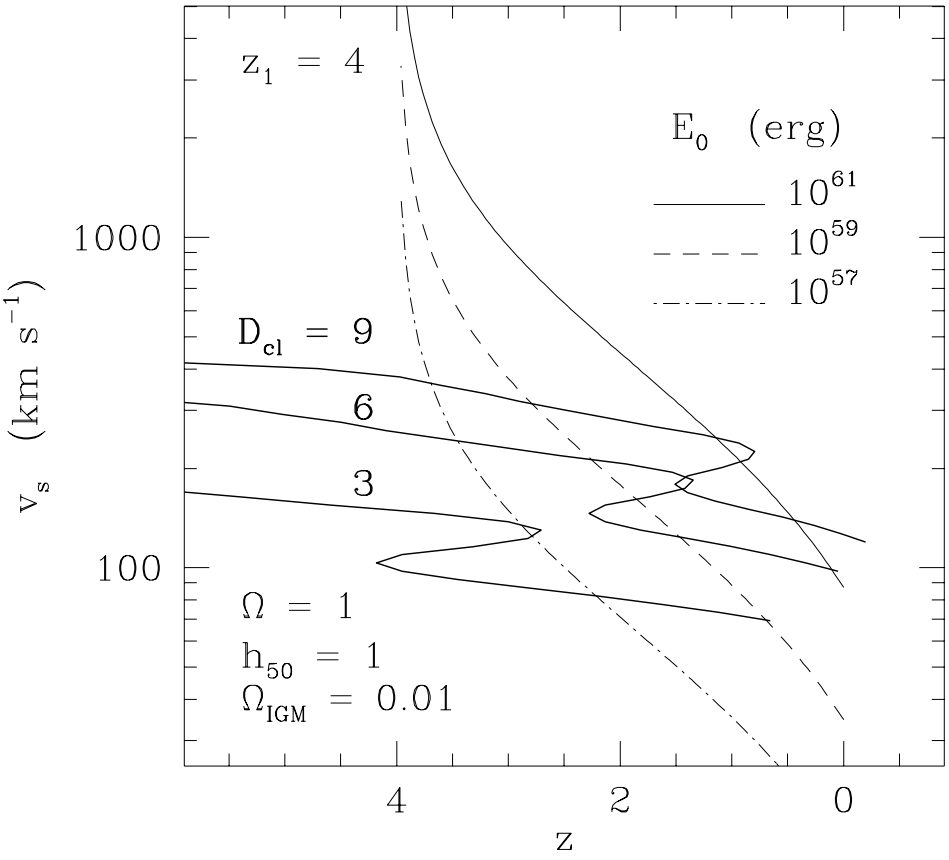

Fig. 11.— Conditions under which shocked clouds cool. Adiabatic shocks that encounter clouds $D_{\rm cl}$ times denser than the ambient IGM can drive radiative shocks into these clouds if $D_{\rm cl}$ is sufficiently large. The heavy solid lines indicate the shock speeds v_s through the ambient medium below which shocked clouds cool in a Hubble time at various redshifts z. Here we show cooling loci for $\Omega = 1$, $h_{50} = 1$, and $\Omega_{\rm IGM} = 0.01$. For reference, we also show $v_s(z)$ trajectories for blastwaves beginning at $z_1 = 4$ with $E_0 = 10^{57}$, 10^{59}, and 10^{61} erg. Because the postshock cooling time is roughly proportional to $D_{\rm cl}^{-2}$, clouds of modest overdensities can cool much more easily than the ambient IGM. Thus, cosmological blastwaves can potentially amplify the neutral column densities of preexisting Lyα clouds by a large factor.